

**University of South Florida**  
***Feasibility, Sustainability and Economic Analysis of Solar Assisted Biomass  
Conversion***  
**(Final Report)**

**PI:** B. Joseph **Co-PI:** Q. Zhang

**Students:** Matt W etherington ( BSCHE), M aria P inilla (MS, C ivil a nd E nvironmental E ngineering),  
Chita Yang (PhD in Chem. Engg.)

**Description:** The main deterrent for commercialization of biomass conversion processes is the cost of conversion; particularly the need to sacrifice as much as 30% of the energy content in the biomass for the thermo chemical conversion step. We want to research and develop the concept to use solar thermal energy from concentrating units to provide energy for the biomass gasification step. We also propose to evaluate the sustainability of such a process.

**Overall Objective:** The overall objective is to conduct a theoretical analysis of solar assisted thermo chemical conversion of biomass from the point of view of energy efficiency, economic feasibility, environmental impact, and long term sustainability of renewable energy production.

**Budget:** \$45,238

**Universities:** USF

## Executive Summary

The overall objective is to conduct a theoretical analysis of thermo chemical conversion of biomass with and without solar energy from the point of view of energy efficiency, economic feasibility, environmental impact, and long term sustainability of renewable energy production.

We completed process design and economic analysis of the thermochemical conversion of biomass to liquids with and without solar energy. It was found that the capital cost of the solar energy collection system is a significant factor in the economics of the process. The cost of solar thermal systems will have to be reduced before solar assisted biomass gasification can become feasible.

Based on economic analysis, the goal of LCA has been shifted to compare different feedstocks and processes because solar assisted biomass conversion is not economically feasible. In this study, a comparative LCA has been developed to evaluate the environmental impacts associated with different energy products via different routes across the whole life of algal and lignocellulosic bioenergy. Results were compared per energy basis, the production of 1 million BTU of energy products. It was found that cultivated algae biomass feedstock has much higher environmental impacts compared with lignocellulosic biomass feedstock from forestation and agriculture byproducts. It was also concluded that thermochemical gasification and FTS process showed higher efficiency when converting biomass to bioenergy.

**University of South Florida**  
**Power Generation Expansion Portfolio Planning to Satisfy Florida's Growing  
Electricity Demands**  
**(Final Report)**

**PI:** Tapas K. Das **Co-PIs:** Ralph Fehr

**Students:** Patricio Rocha (Ph.D. graduated August 2011), Felipe Feijoo (Ph.D.)

**Description:** The objectives of the proposed research are to 1) develop a comprehensive generation technology based portfolio optimization (GTPO) model and its solution algorithm, and 2) develop educational resources to enhance training of scientific workforce for the state of Florida. The research will directly address three major challenges: fulfillment of the growing power demand, meeting the emissions targets, and supply of technology workforce. The potential economic impact of the proposed research on the State of Florida is expected to be very high, since an energy-secure environment is a basic necessity to support the current trend of explosive growth both in industry and human resources.

**Budget:** \$ 71,906

**Universities:** USF

**External Collaborators:** Argonne National Laboratory (not funded by this project)

## EXECUTIVE SUMMARY

The first phase of the project was focused on the generation capacity expansion aspect of the electricity networks. We begin the executive summary by providing the title and the abstract of that study. A detailed report on the Phase I is provided as a separate document. Phase II of the project focused on the cap-and-trade policy designs for carbon emissions reduction. In the rest of the executive summary, we provide details of our findings from this phase.

### Phase I:

Title: Impact of CO<sub>2</sub> Cap-and-Trade Programs on Restructured Power Markets with Generation Capacity Investments

**P. Rocha**

PJM Interconnection  
Norristown, PA, USA 19403

**T. K. Das**

University of South Florida,  
Tampa, Florida, USA 33613

**V. Nanduri**

University of Wisconsin-Milwaukee,  
Milwaukee, Wisconsin, USA 53201

**A. Botterud**

Center for Energy, Environmental, and Economic Systems Analysis,  
Argonne National Laboratory,  
Argonne, Illinois, USA 60439

## Abstract

A cap-and-trade program is the most widely discussed policy aimed at achieving CO<sub>2</sub> emissions reductions. Since power plants in the U.S. and other industrialized nations are responsible for a sizable portion of CO<sub>2</sub> emissions, the implementation of a CO<sub>2</sub> cap-and-trade program will have a significant impact on the power generation sector. Assessing this impact is a challenging task, especially in restructured electricity markets. Cap-and-trade programs consider multiple design parameters and attributes as well as the creation of a new market for CO<sub>2</sub> allowances, all of which will affect the capacity investment decisions of generators and the bids that generators submit to the day-ahead and real-time electricity markets. In this paper, we develop a game theoretic model driven methodology to assess the impact of CO<sub>2</sub> cap-and-trade programs in restructured electricity markets. The methodology is implemented on a sample power network created from the electricity market data of northern Illinois in the U.S. The network is assumed to operate under a CO<sub>2</sub> cap-and-trade program similar to the Regional Greenhouse Gas Initiative (RGGI). The impact of cap-and-trade policy on the equilibrium generation expansion plan and the electricity market operation is examined via variations in prices, CO<sub>2</sub> emissions, demand, and evolution of technology mix in the generation portfolio over a planning horizon.

### Phase II:

Title: Pareto Optimal Designs for CO<sub>2</sub> Cap-and-Trade Policies in Deregulated Electricity Networks

**Felipe A. Feijoo and Tapas K. Das**

Department of Industrial and Management System Engineering  
University of South Florida, 4202 E. Fowler Avenue, Tampa, FL 33620

## Abstract

Economic studies have shown that CO<sub>2</sub> emission reduction programs are likely to have adverse effects on the electricity network performance (e.g., rise in LMPs). Among the CO<sub>2</sub> emission reduction programs, cap-and-trade (C&T) is the most widely used strategy. Current research on C&T policies can be categorized into models for allowance allocation (no-cost allocation based on emissions history or via auction) and empirical economic studies for examining impact on network performance. This paper presents a mathematical-statistical approach to develop Pareto-optimal designs for CO<sub>2</sub> C&T policies by examining the combined impact of policy design parameters (initial allowance cap, cap reduction rate, violation penalty) on various measures of network performance. Measures that are considered are social welfare and the corresponding system marginal cost or price (MP), CO<sub>2</sub> emissions, and electricity production level. The model has two layers: top layer involves design of optimal cap-and-trade policy parameters over a planning horizon, and the bottom layer involves finding equilibrium bidding strategies of the competing generators while maximizing social welfare via DC-OPF. In the bottom layer, for each competing generator, we formulate a bi-level mathematical model, where the upper level focuses on maximizing generator profit through bids to ISO in both allowance and electricity markets. The lower level focuses on social welfare maximization while meeting the network and policy constraints. We reformulate each bi-level problem as a mathematical problem with equilibrium constraints (MPEC). The equilibrium bidding behavior among the competing generators is obtained by solving the set of MPECs as an equilibrium problem with equilibrium constraints (EPEC). For the top layer, we use a statistical (designed experiment) approach to examine the impact of individual C&T policy parameters on network performance (obtained from the bottom layer). This yields regression models linking policy parameters to each network performance measure. Finally, a multi-objective optimization approach is used to develop the Pareto optimal cap-and-trade designs.

***Solar Photovoltaic Manufacturing Facility to Enable a Significant Manufacturing Enterprise within the State and Provide Clean Renewable Energy  
(Progress Report)***

**PI:** Don L. Morel **Co-PI:** Chris Ferekides, Lee Stefanakos

**Students:** K. Jayadevan (MS), S. Bendapudi (MS 5/11), R. Anders (PhD), Y. Wang (PhD), Manikandan Sampathkumar (MS)

**Description:** The primary goal of this project is to enable the establishment and success of local solar photovoltaic manufacturing companies to produce clean energy products for use within the state and beyond and to generate jobs and the skilled workforce needed for them. Thin film technologies have shown record efficiencies of 20%, and present tremendous opportunities for new Florida start-up companies. USF, UCF, and UF are collaborating to develop a pilot line facility for thin film solar technologies, which will serve as a test bed for making ongoing improvements in productivity and performance of solar modules, develop advanced manufacturing protocols, and help train a skilled workforce to ensure the success of new companies.

**Budget:** \$1.6M

**Universities:** USF, UCF, UF

**External Collaborators:** Mustang Solar, a Division of Mustang Vacuum Systems

**Summary of Annual Progress**

Over the past year progress has continued to be made on the two main tasks of the project, development of the Thin-Film Pilot Line deposition system and development and advancement of laboratory scale processes for CIGS related materials and devices. As a result of the changing landscape related to CIGS manufacture the Pilot Line System was modified to focus on the key elements currently controlling commercialization of the technology. Simulation tools that address cost factors as well as technology were developed and utilized to guide the redirection of the design. It was determined that deposition rates of 20 Å/s and above were needed to hit the targeted cost factors for capital equipment utilization. The design of the deposition machine and the process recipes will allow attainment of these rates.

The key factor for machine and process design on the technology side is the arrival rate and sequence of the CIGS constituents. Simulation tools have been developed and utilized that allow determination and control of these species. The deposition tool set utilizes two pair of metal deposition sources and several Se sources distributed over the deposition zones. The two-dimensional deposition profile of the components are individually simulated and then combined to simulate the overall two-dimensional profile. Imbedded in the simulations is the ability to control the evolution of the metal ratios across the deposition zone. And, simulation of the Se/metal profiles within a targeted range completes the capture of the entire deposition process. The insights provided from these simulations have guided the design of the deposition system. It will be versatile enough to enable access to a large range of deposition space that contains the

optimum parameters for performance and cost control. The machine components have been delivered, and it is currently being assembled.

Based upon CIGS laboratory scale experimentation that has been underway two process recipes have been chosen to implement in the Pilot Machine. The initial configuration of the machine will be directed toward determining which of these has the most potential for success. On a longer timeframe we have also been developing CuZnSnSe (CZTS) as a sustainable substitute for CIGS. With increasing production volume the availability of In may drive up its cost. CZTS uses earth abundant materials and has demonstrated efficiency in the 10% range. We have been developing the material, and with new insights gained from use of Raman spectroscopy have made significant progress in improving material quality. Initial results from devices made with the upgraded material are also promising.

### 3.0 Thin Film Pilot Line

As progress is being made in the manufacture of CIGS solar panels new challenges and opportunities are emerging for ongoing growth of the technology. Champion large area module efficiencies of 16% are being reported, and average production efficiencies are catching up. So it is clear that performance parameters for large scale applications can be met. What remains is to demonstrate that costs are competitive and have a pathway to remaining so. The key to cost is throughput and materials utilization. These translate to fast deposition rates and management of In and Ga utilization. From the beginning of our research endeavors at USF we have always pursued deposition technologies that would be able to pass commercialization muster while avoiding those that allowed fast pathways to high efficiency, but had no chance at commercialization. There has been a series of companies that failed by trying to commercialize the easy high efficiency technologies. With this backdrop we have designed our new deposition system to accommodate the commercialization drivers. The system will incorporate tools to evaluate deposition approaches that have not been reported in the literature. Our objective is to demonstrate that one of these surpasses commercialized technologies in performance and cost.

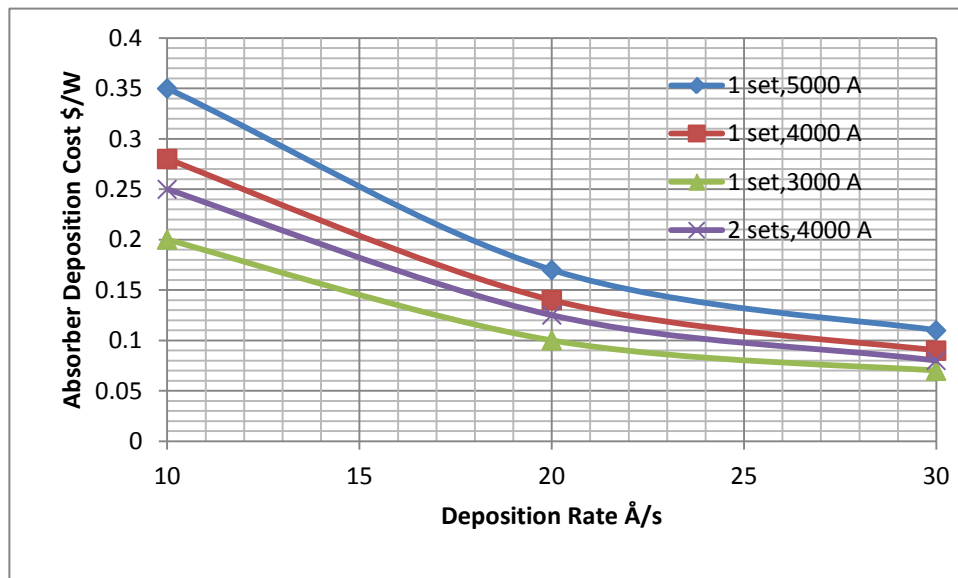


FIGURE 5. PROJECTED CAPITAL EQUIPMENT COST IN \$/W FOR CIGS DEPOSITION AS A FUNCTION OF DEPOSITION RATE

## Cost Simulation

Throughout the project we have developed and used simulation tools to guide our technology development. Of particular importance to the design of the deposition system is the projected capital cost/Watt for the deposition tool. The drivers for this cost factor are the capital cost of the equipment, the throughput, the efficiency and the yield. There are also variations for series and parallel target configurations that have various cost tradeoffs. An example of results for a few of these configurations is shown in Fig. 1. This component for the cost of a finished module should be about 20%, which for a selling price of \$0.60/W should be around \$0.12/W. As can be seen in the figure, this threshold can be reached for deposition rates of 20 Å/s and higher.

At this point it is necessary to bring another technical factor into the cost discussion. Deposition rates of 20 Å/s can be attained by both sputtering and thermal evaporation of the source materials. While thermal evaporation is the technology that has been used to progress efficiencies to the 20% level, it has not proven to be a successful technique for large area manufacturing. Sputtering is considered the technology of choice for large area manufacture because of its ability to deposit uniformly and reproducibly over large areas. Ideally one would like then to just sputter from a CIGS target or maybe a combination of CuSe, In<sub>2</sub>Se<sub>3</sub> and Ga<sub>2</sub>Se<sub>2</sub> targets. These approaches have not worked largely because of loss of Se, but even if they did, sputter rates of 20 Å/s and higher are not realistic for “ceramic” targets. Thus sputtering of metals is what must be pursued, and that is what we, and others, are working at. Depositing Cu, In and Ga at these rates is not the problem, it is rather how to selenize the metal layers. This is where innovations are needed to enable the emergence of this technology and what is guiding our efforts and the design of our deposition tool.



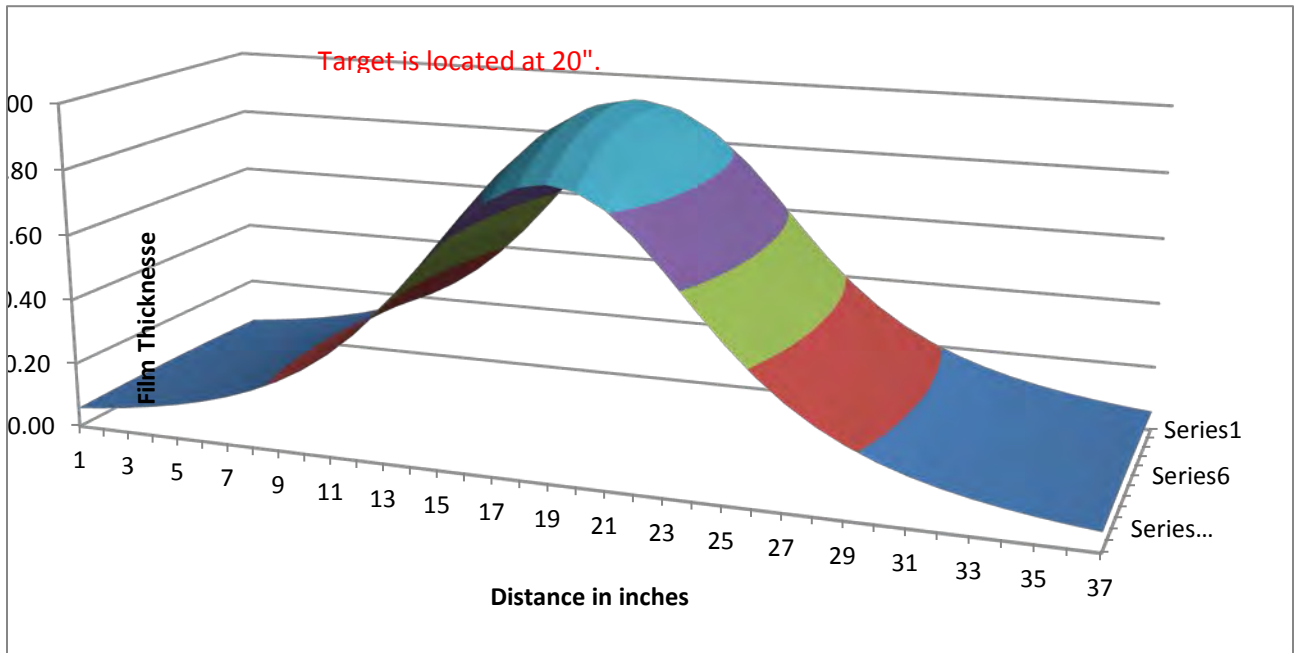


FIGURE 6. THICKNESS PROFILE OF A SPUTTERED FILM ON THE WEB.

### Deposition Simulation

The process recipes that we will be developing are based upon sputtering of the metal components. We will pursue a couple of different approaches to Se delivery and determine which is most effective. The deposition system will be in a roll-to-roll configuration and will be able to handle “plastic” as well as stainless steel coils. The width of the substrate will be 4”. Champion efficiency cells are made in deposition systems on small substrates onto which all four components, Cu, In, Ga and Se

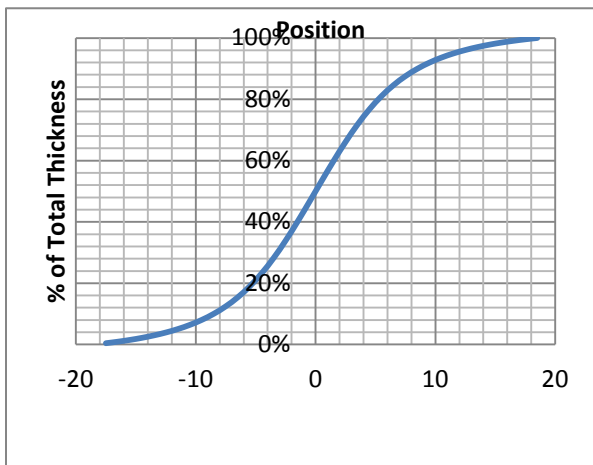


FIGURE 3. CUMULATIVE THICKNESS AS A FUNCTION OF WEB POSITION.

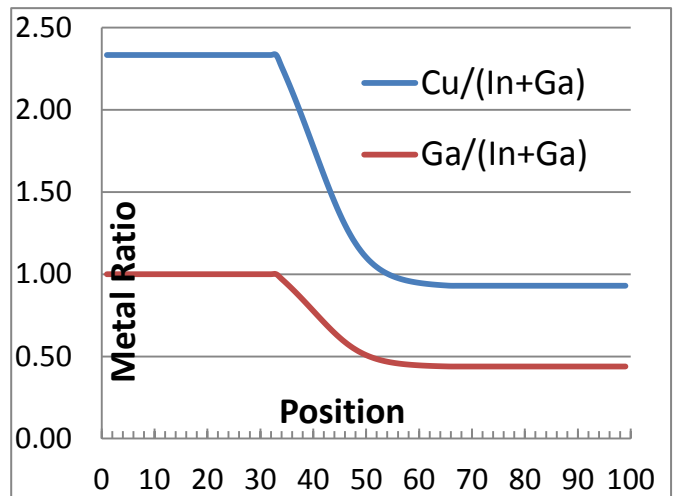


FIGURE 4. METAL RATIO PROFILES FROM FOUR SPUTTERING SOURCES.

are delivered to the substrate simultaneously and carefully controlled. This is not possible in a manufacturing scale system based upon sputtering.

In these systems the components are delivered to a moving substrate by multiple sputtering sources. Consequently there are time offsets in the arrival of the constituents. Given the complex phase space of CIGS and the potential for formation of unfavorable phases it is important to understand the formation chemistry and to design the deposition tools to be able to access the region of deposition space that produces high quality, single-phase CIGS. Throughout the years we have explored and studied many regions of this phase space and have designed the deposition tool to access regions that we know to be viable. To effectively use this understanding we have developed deposition simulation tools to guide design of the deposition tools. Figure 1 shows the instantaneous thickness profile, or equivalently the flux, of the deposition along the web for a sputter target located at 20". Fig. 3 shows the resulting thickness increase as the web moves over the sputtering source. There is a corresponding profile for a second sputter source adjacent to the first one. It has the same profile, but offset from the first source. Thus the instantaneous composition at any location on the web can be determined. Further, the composition can be changed by adjusting the separation distance between the sources, the sputter gun angle and the deposition rates. Fig. 4 is an example of the emergence of the metal ratio profile as a function of position for four sputtering sources resulting in targeted ratios of 0.9 for Cu/(In + Ga) and 0.4 for Ga/(In + Ga).

In addition to controlling the metal fluxes it is important to attain the proper delivery profile for Se. It is necessary to have an overpressure of Se to achieve full selenization of the films. A simulation result for one of the two pairs of sputter sources used for the Fig. 4 simulation is shown in Fig. 5. The targeted ratio of Se/metal is 3 – 5. The red(top) curve in the figure is this ratio and indicates that the desired range is achieved. The underlying curves are the contributions from the individual sources.

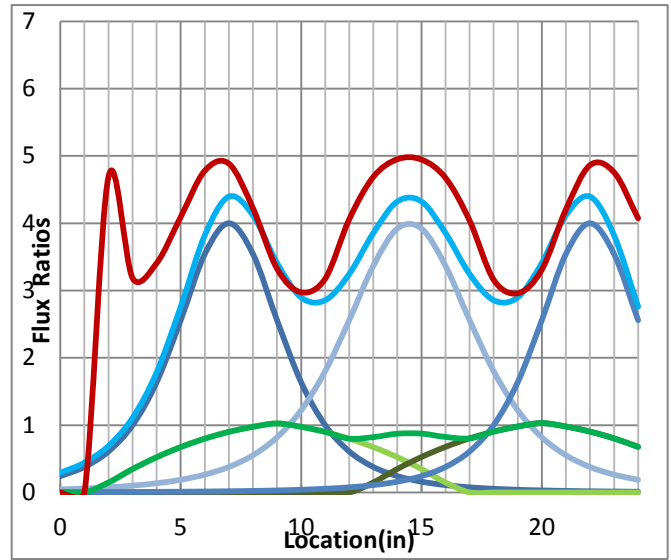


FIGURE 5. FLUX RATIOS FOR TWO SPUTTER SOURCES AND SE SOURCES.



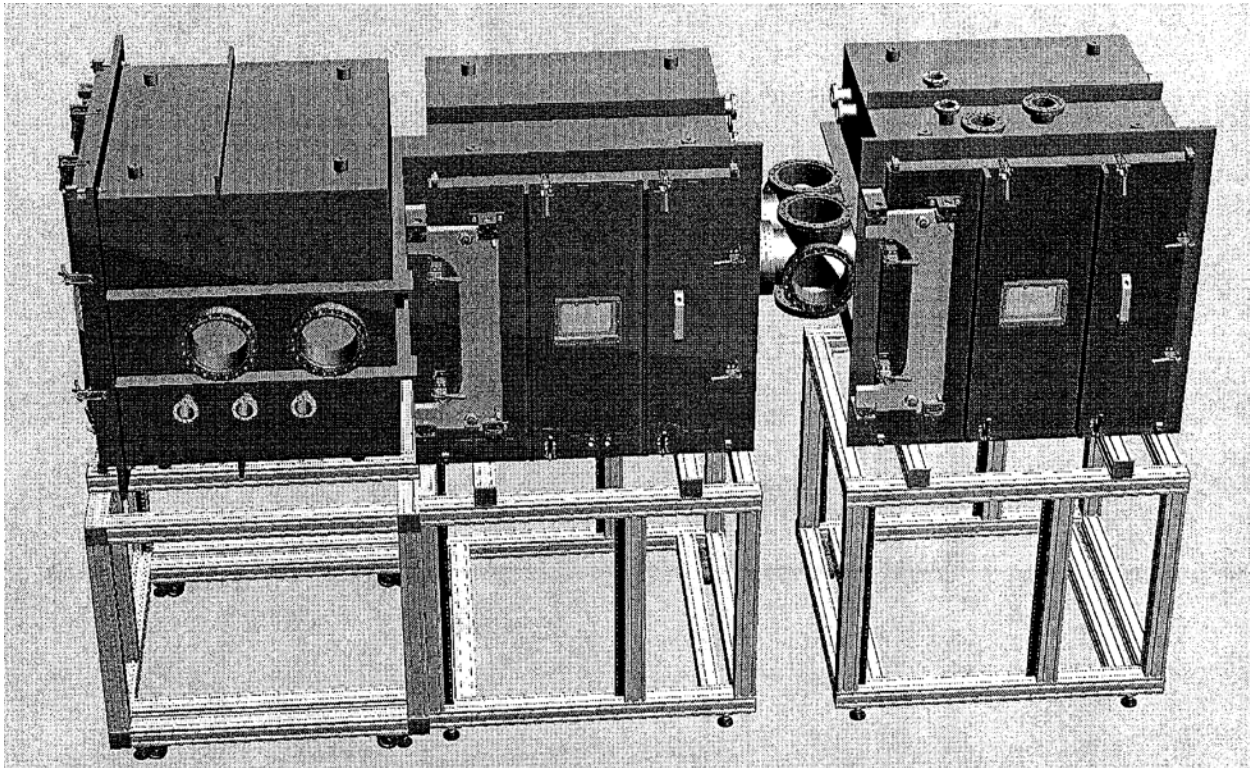


FIGURE 7. PILOT-LINE DEPOSITION SYSTEM.

The insights gained from the above analysis were used to guide the development of the Pilot-Line de position s y s t e m s h o w n a b o v e w h i c h h a s a t o t a l l e n g t h o f 10 f e e t . T h i s f i g u r e i s b e f o r e a l l o f t h e o p e r a t i o n a l h a r d w a r e h a s b e e n i n s t a l l e d . W e h o p e t o r e p o r t n e x t t i m e o n i n s t a l l a t i o n a n d o p e r a t i o n o f t h e s y s t e m a n d i n i t i a l r e s u l t s .

### Sustainable Materials

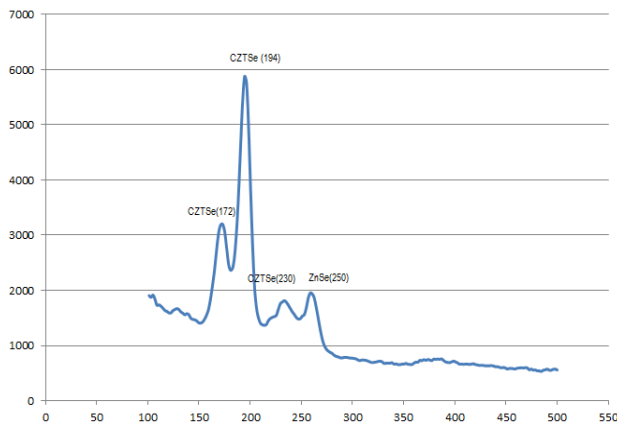


FIGURE 9. RAMAN SPECTRUM OF CZTS.

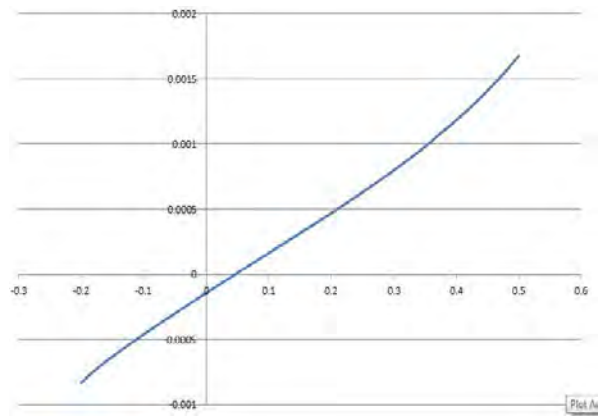


FIGURE 8. CZTS IV CURVE.

One of the cost issues for CIGS is Indium. It is currently available and cost-effective, but going forward to large volumes this might not remain true. Consequently we and others have been pursuing alternative CIGS-related compounds. In particular we have focused our efforts on CuZnSnSe. Efficiencies of 5 – 10% have been reported for CZTS made with different techniques. We have chosen a deposition pathway that we believe will meet the requirements for large scale manufacture. Our efforts thus far have concentrated on attaining good materials properties. This material is more complex than CIGS because of the various locations that the metals can take in the lattice. These properties are also difficult to characterize by the usual techniques of XRD because of the similarities of the fingerprints for the relevant phases. We developed an optical technique which was reported previously<sup>1</sup> and which was helpful in identifying the presence of ZnSe. Our attempts at making devices were being thwarted by the formation of ZnSe. Recently we started using Raman spectroscopy to gain further insights to the structural composition of our material. In Fig. 7 we show a Raman spectrum for a sample made at an annealing temperature of 300 °C. The main peak at just under 200 cm<sup>-1</sup> is that of CZTS with two satellite peaks on either side. The peak at 265 cm<sup>-1</sup>, although identified to be ZnSe, is more likely CuSe. With additional processing at higher temperatures we find that this peak disappears. It is known that CuSe forms at lower temperatures and then reacts with the other constituents to form CZST. We are using these insights to guide further development of our material and believe that the electronic quality is now significantly better. However, the ultimate proof of material quality is in device performance. We have started making devices with the upgraded materials process and are seeing encouraging results. An IV curve of a device showing PV response is shown in Fig. 8. Once we advance the performance of CZTS at the laboratory level, we can also transfer the process to the Pilot-Line machine for further development.

<sup>1</sup> Y. Wang, S. Bendapudi, C. S. Ferekides and D. L. Morel, “*Optical Determination of Phase Composition and Processing Effects on Cu<sub>2</sub>ZnSnSe<sub>4</sub> Film Quality and Device Performance*”, Proceedings of the 38<sup>th</sup> IEEE PV Specialist Conference, Austin, June, 2012.

## University of South Florida

### *Sustainable Algal Biofuel Production*

#### (Final Report)

**PI:** Sarina J. Ergas    **Co-PI:** Qiong Zhang, James R. Mihelcic, John Wolan (deceased)

**Students:** Angela Chapman, PhD Secondary Education in progress; Matthew Gaston, MS Environmental Engineering in progress; Benjamin Gillie, BS Chemical Engineering; Trina Halfhide, PhD Engineering Science in progress; Mehregan Jalalizadeh, MS Environmental Engineering; Ruben Jean, BS Environmental Engineering (UF) in progress; Eunyong Lee, PhD Environmental Engineering in progress; Maria Pinilla, MS Environmental Engineering; John Trimmer, MS Environmental Engineering in progress; Innocent Udom, PhD Chemical Engineering in progress; Sarah Watson, MS Environmental Engineering in progress.

**Description:** Microalgae are productive at utilizing CO<sub>2</sub> and can generate biomass for production of biodiesel, methane, or other fuels as well as valuable co-products (e.g. animal feeds, polymers). Algal biofuel production can be more profitable and sustainable when combined with wastewater treatment and CO<sub>2</sub> utilization from electric power generation facilities. A number of research gaps exist for full scale algal biofuel production including: 1) improvement of algal growth and nutrient uptake rates, 2) integration of systems with waste gas, wastewater, and water reclamation systems, 3) improved gas transfer and mixing, 4) improved algal harvesting and dewatering and 5) life cycle assessment (LCA) and economic analysis. In addition, little attention has been given to the potential use of algal biofuel systems to treat wastewater and produce heating and cooking fuels in developing countries. The overall objective of this project is to develop an interdisciplinary multi-investigator research program that integrates microalgal biofuel production with wastewater treatment and carbon recycling. An algal biofuels lab will be established at the USF Botanical Gardens, which will house several bench-scale algal photobioreactors. Initial experiments will focus on optimizing CO<sub>2</sub> uptake from combustion gases, wastewater nutrient removal and production of algal biomass under varying operating conditions. Both oil rich algal species and algae that grow well on wastewater will be investigated. LCA methods will be used to provide insight into the environmental impacts of the process under varying conditions and enable system evaluation based on both technical performance and life cycle impacts. This project is designed to develop PI expertise and collaborations and train graduate students in a new field of research that is critical in establishing Florida as center of algal biofuels production. Future research directions include: 1) integration of algal biofuel production with domestic, agricultural and industrial wastewater, 2) sustainable aquaculture system development, 3) production of jet fuel from algae cake, 4) application of algal biofuels technology in developing countries, 5) development of integrated LCA-economic assessment tools to assist in algal biofuel system decision making.

**Budget:** \$50,000

**Project Time Period:** 2/1/2010-6/30/2012

**Universities:** USF

**External Collaborators:** Mote Marine Laboratories

## Updated Executive Summary:

Algae can be used to produce a range of fuels (biodiesel, biogas, liquid hydrocarbon fuels) while mitigating CO<sub>2</sub> and nutrients. However, critical research gaps remain for the development of full-scale sustainable photosynthetic microalgal biorefineries. The overall goal of this project is to transform microalgal bioenergy production from the status quo to an economically and environmentally sustainable state through improvements and optimization across the life cycle of microalgal cultivation and harvesting stages. Specific objectives were to:

1. increase the productivity of algae and their intracellular storage products through bioprospecting and phototrophic culture development,
2. reduce water and material input through integration of municipal and aquaculture wastewater treatment with algal cultivation,
3. improve nutrient, CO<sub>2</sub>, and light delivery through improvements in gas transfer and mixing,
4. reduce downstream processing and energy costs through improvements in harvesting technologies,
5. apply system level modeling and life cycle assessment to optimize energy production while assuring environmental and economic sustainability; and
6. integrate students from a disadvantaged high school into the project as authentic researchers.

Wild algae were harvested from secondary clarifiers of wastewater treatment facilities and tested for algal growth and nutrient uptake rates on:

1. municipal wastewater from the Glendale (Lakeland FL) treatment facilities,
2. sludge centrate from the Howard F. Curren Wastewater Treatment Facility in Tampa,
3. sludge centrate from pilot-scale anaerobic digesters treating swine wastes at USF,
4. aquaculture wastewater from Mote Aquaculture Park (Sarasota FL).

An algal biofuels laboratory was established at the USF Botanical Gardens. The lab was used to conduct pilot-scale photobioreactor studies of algal growth on municipal sludge centrate over a two year period. Algae collected from the reactors were used in harvesting studies to determine the effectiveness, costs and life cycle environmental impacts of different harvesting technologies. Additional modeling studies were used to investigate the feasibility of integrating algal biofuel production with recirculating aquaculture systems. High school students were included as authentic researchers through a collaboration with a biotechnology and marine science teachers at a Middleton HS, a STEM magnet school in Tampa that serves a historically African American and economically disadvantaged neighborhood. Our current work is focused on culturing algae on anaerobically digested animal manure and aquaculture wastewater, anaerobic co-digestion of algae and life cycle assessment studies.



*Development of a Highly Efficient Photocatalyst for CO<sub>2</sub> Reduction with H<sub>2</sub>O by Hybrid Construction of Transparent, Conductive Composite (TCC) and nano-Sized MOX/INVO/AL<sub>2</sub>O<sub>3</sub> Particles*

**PI:** Norma Alcantar, John Wolan (deceased)

**Description:** Our research focused on three technologies to produce films able to respond to external stimuli. We used conductivity as the intrinsic property that was a prime parameter to consider when performance was measured. We also were interested on the fundamental structure that would make our conducting films and materials to enhance their performance.

**Project Time Period:** 2/1/2009-6/30/2011

**Universities:** Department of Chemical and Biomedical Engineering, USF

**External Collaborators:** Mote Marine Laboratories

### Executive Summary

This project's goal was to prepare transparent conductive composites (TCCs) in which organic and inorganic materials were used to produce and characterize a complex material with smart capabilities. Our research had a direct impact in battery production, conducting films and catalysis.

### Goals and Objectives

- 1) Determine protocols for synthesis of conductive composites
- 2) Determine performance
- 3) Characterize their structure
- 4) Measure efficiency

### Research Description

Our research focused on three technologies to produce films able to respond to external stimuli. We used conductivity as the intrinsic property that was a prime parameter to consider when performance was measured. We also were interested on the fundamental structure that would make our conducting films and materials to enhance their performance.

The following is a description of the main accomplishments of this research.

- a) Conductive polymer complexes were prepared by doping optically transparent polymers with bis(ethylenedioxy)-tetrathiafulvalene (BEDO-TTF) and then exposing such films to iodine (anion donator) to form a conducting crystalline surface with the potential for sensing. Our research determine that once polymeric films are doped and exposed to an anion donator, their surface structure is affected by undergoing changes from amorphous to crystalline accommodations as shown in the following Figure.

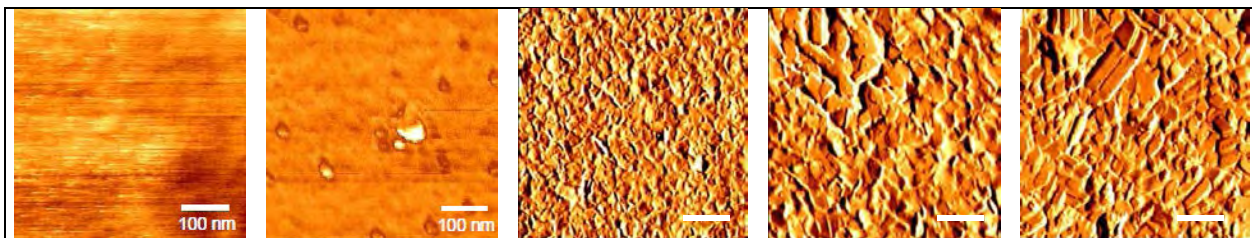
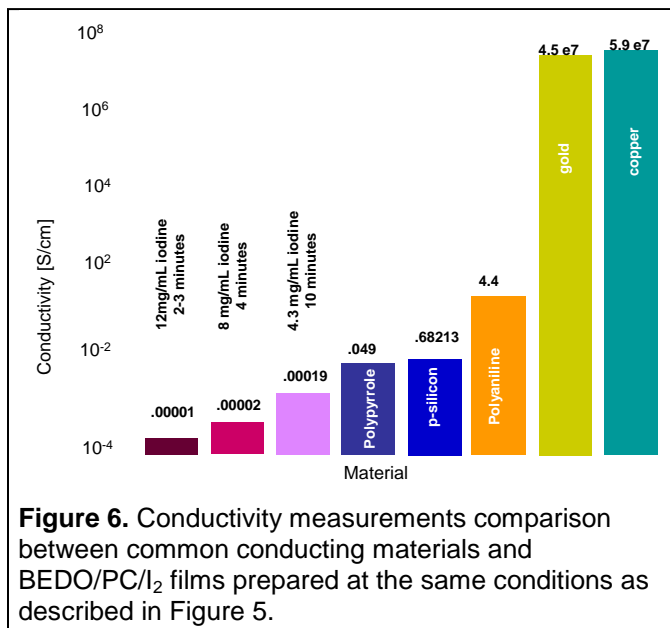


**Figure 1.** Phase contrast AFM scans: Bare PC (A), BEDO/PC (B), BEDO/PC/1mg/ml-2min exposure to Iodine (C), BEDO/PC/8mg/ml-4min Iodine (D), BEDO/PC/4.3mg/ml-10min Iodine (E). The scan size of A & B is 0.5x0.5µm. The scan size of C, D & E is 5x5µm, scale bar depicts 1µm. High resolution scans for A & B are shown intentionally to discern structure differences due to dye-doping as compare to C, D & E.

Data comparing common conducting materials to BEDO/PC/Iodine films are shown in Figure 2. Our data shows that the film conductivity is high if the coverage is uniform. Consequently, the films need to be exposed to low concentrations of  $I_2$  for longer periods of time. It is also clear that structure and conductivity are related. The film with ordered-crystalline structure reported the highest conductivity (Fig. 1E), while the film with amorphous structure reported poor conductivity (Fig. 1C). The surface of the composite films becomes conductive as a result of complex formation between acceptor ( $I_2$ ) and donor species from BEDO-TTF. The reverse side of the same film is non-conductive. Hypothesis I in this proposal focuses on controlling surface structure at the nano and micron level. These initial measurements have encouraged further work on optimizing conductivities through correlation to crystal morphologies.



We have submitted a proposal to NSF. Our first attempt was unsuccessful but we will resubmit with comments to the reviews in the next funding cycle.

- b) Our second technology included the production of flexible aluminum and hydrogen peroxide galvanic cells by encapsulating the oxidizer. In this work, we found that the side reactions can be diminished by controlling the cathodic reactant using micelles (non-ionic surfactant vesicles) and polymeric networks. Results indicate an average energetic output value of  $0.57 \pm 0.09$  KJ vs.  $0.54 \pm 0.05$  KJ without the implementation of the cathodic encapsulation system. In addition, we also found that composition of the aluminum electrode was decreased by 15%, which could then translate in 79% in savings according to the market price of aluminum and savings on the secondary reactions.
- c) The third technology included the use of  $MO_x/InVO_4/Al_2O_3$  photocatalysts (both in the UV or visible range) to eliminate off-flavor compounds in recirculating aquaculture systems (RAS). Heterogeneous photocatalysis is a process in which a solid semiconductor catalyst (e.g. titanium dioxide) absorbs light and subsequently initiates the degradation of chemical compounds through direct surface interaction or generation of oxidizing species such as hydroxyl radicals. A major benefit of photocatalysis is that the pollutants are destroyed and not simply transferred to another phase as in the case of activated carbon or membrane processes. In addition, it is much less





Florida Energy Systems Consortium

expensive than using one, which requires on site generation and the setup of expensive equipment.

### Concluding Remarks

Our project has made a significant impact in current research areas of national interests. It has branched out into multidisciplinary applications and it has implications in biosensing, environmental science, water purification, and fundamental research involving novel battery systems.

### Patents

8,034,302      Transparent conducting composites (TTCs) for creating chemically active surfaces

### Publications

Novel Encapsulation of Oxidizer Applied to Galvanic Cells: Aluminum / H<sub>2</sub>O<sub>2</sub> Galvanic Cell as a Case Study by Marlyn Colon to obtain her Masters of Science Degree in Chemical Engineering, University of South Florida (2011). <http://scholarcommons.usf.edu/cgi/viewcontent.cgi?article=5213&context=etd>

Characterization of conductive polycarbonate films by Selma Hokenek to obtain her Masters of Science Degree in Chemical Engineering. University of South Florida, (2009)

Other publications are in the process of being sent out for review.

<http://scholarcommons.usf.edu/cgi/viewcontent.cgi?article=3015&context=etd>

Other publications are in the process of being submitted.



**University of South Florida**  
***Development of a Smart Window for Green Buildings in Florida***  
**(Final Report)**

**PI:** Dr. Sarath Witanachchi

**Students:** Mr. Mark Merlak, Ph.D. student

**Description:** The microwave plasma system was used to grow nanophosphors of La<sub>2</sub>O<sub>3</sub>:Bi and CaS:Eu. The system was modified to accommodate chemical vapor deposition (CVD) of ZnO and ZnS. ZnO coatings were grown by introducing zinc acetylacetonate (Zn(acac)<sub>2</sub>) vapor as precursor near the substrate. Vapor was generated by heating granules of Zn(acac)<sub>2</sub> in a container to 160°C and pushing the vapor with gas that contained a mixture of Ar and oxygen. Methylzinc and H<sub>2</sub>S were used for the growth of ZnS films.

Microwave plasma process allows control of nanophosphor particle sizes by controlling the precursor concentration. We have demonstrated the ability to deposit La<sub>2</sub>O<sub>3</sub>:Bi nanophosphors in single crystal form with sizes from 5nm to 100 nm by changing the starting concentration. Transmission Electron Microscopy (TEM) showed the hexagonal crystals and clear lattice planes with  $d=3.34\text{\AA}$  that corresponds to (100) orientation. BTO layer required for the device structure was sputter deposited at low temperature.

Radiant flux emitted by devices fabricated with the conventional EL structures and devices with the proposed structures were measured by the integrated sphere technique. Measured values confirmed the enhancement in emission resulting from the proposed structure. The observed upward trend confirms the viability of the concept and the potential of EL devices fabricated under optimum conditions to reach desired outputs of 1300-1500  $\mu\text{W}$  (13-15 W/m<sup>2</sup>).

**Executive Summary:**

This project is aimed at developing a smart window concept that has the potential to convert part of the solar radiation falling on windows during daytime to electricity, and to use this harnessed energy to power a phosphor-based, highly efficient white-light LED source to illuminate the building at night. This project pursues two different technologies: (1) use of quantum dot based solar cells to harvest solar energy, and (2) develop an electroluminescent light source based on nanophosphors to provide illumination for buildings. The project brings together two unique nanoparticle growth techniques developed at the Laboratory for Advanced Material Science and Technology (LAMSAT) at USF to fabricate a prototype device that would demonstrate the possibility of significant energy savings. Research accomplishments related to solar device was presented in last annual report. This report focuses on research developments in the solid state lighting device.

### *High Efficiency Black Polymer Solar Cells (Progress Report)*

**PI:** Dr. Franky So

**External Collaborators:** John Reynolds, Georgia Tech

**Industry Partner:** Sestar Technologies, LLC

**Students:** Cephas Small and Song Chen

**Description:** The objective of the proposed project is to synthesize broadly absorbing, black colored (PBLACK) polymers with especially high charge mobilities and to fabricate the highest performance polymer solar cells possible. Specifically, we will synthesize polymers with absorption band ranging from 400 nm to beyond 1  $\mu\text{m}$  with carrier mobilities higher than  $10^{-4}$   $\text{cm}^2/\text{Vs}$ . Polymer-fullerene (both PC<sub>60</sub>BM and PC<sub>70</sub>BM along with more recently developed derivatives) blend morphology will be optimized using different solvent/heat treatments as well as additives to the blends. The final device will be enhanced using anode and cathode interlayers to enhance carrier extraction to the electrodes. With the ability to synthesize broadly absorbing polymers, control the donor-acceptor phase morphology and engineer the device structure, it is expected that the power conversion efficiency of polymer solar cells can reach 10% at the end of the two-year program.

#### Summary of Progress

Polymer bulk heterojunction solar cells based on low bandgap polymer:fullerene blends are promising for next generation low-cost photovoltaics. While these solution-processed solar cells are compatible with large-scale roll-to-roll processing, active layers used for typical laboratory-scale devices are too thin to ensure high manufacturing yields. Furthermore, due to the limited light absorption and optical interference within the thin active layer, the external quantum efficiencies (EQEs) of bulk heterojunction polymer solar cells are severely limited. In order to produce polymer solar cells with high yields, efficient solar cells with a thick active layer must be demonstrated. In this work, the performance of thick-film solar cells employing the low-bandgap polymer poly(dithienogermole-thienopyrrolodione) (PDTG-TPD) was demonstrated. Power conversion efficiencies over 8.0% were obtained for devices with an active layer thickness of 200 nm, illustrating the potential of this polymer for large-scale manufacturing. Although an average EQE > 65% was obtained for devices with active layer thicknesses > 200 nm, the cell performance could not be maintained due to a reduction in fill factor. By comparing our results for PDTG-TPD solar cells with similar P3HT-based devices, we investigated the loss mechanisms associated with the limited device performance observed for thick-film low-bandgap polymer solar cells.



Florida Energy Systems Consortium

## 1. Funds leveraged / New Partnerships Created

New collaborations						
Partner name		Title or short description of the collaboration			Funding, if applicable	
Proposals						
Title	Agency	Reference Number	PI, Co-investigators and collaborators	Funding requested	Project time frame (1 year, 2 years, etc.)	Date submitted
Dipole Engineering for polymer solar cells	DOE Basic Energy Science		Franky So (UF) John Reynolds (Georgia Tech)	\$840,000	3 years	November, 2012
Grants Awarded						
Title		Agency	Reference Number	PI, Co-investigators and collaborators	Period of Performance	Funding awarded

### 2013 Annual Report

#### High efficiency polymer solar cells with thick films and prototypical structure for printing

Based on the demonstration of high efficiency polymer solar cells based on a low bandgap donor-acceptor copolymer with alternating di-thienogermole-thienopyrrolodione (DTG-TPD) repeat units last year, we further present high efficiency inverted polymer solar cell with thicker active layers that will potentially facilitate the production yield of roll-to-roll printing process. One key factor for improving the large-scale R2R processing compatibility of polymer solar cells is the active layer thickness required to ensure high manufacturing yields in PV modules. Most high efficiency laboratory-scale devices demonstrated have an active layer with a thickness of about 100 nm which is too thin for R2R processing to ensure a pinhole-free film. Obtaining high efficiency devices with active layers thicker than 200 nm is critical for commercialization. To achieve high efficiency with an active layer thickness larger than 200nm, we fabricated the device containing a bottom transparent oxide electrode, a ZnO-PVP composite layer with UV-ozone treatment, a photo-active layer composed of P-DTG-TPD and fullerene, a layer of molybdenum oxide and a top electrode—silver. In addition, the efficiency loss mechanism in the thick devices was studied in depth by the measurement of field dependent external quantum efficiency spectra and photoconductivity analysis. The work is done in collaboration with Dr. John Reynolds at Georgia Institute of Technology.

**Figure 1** shows the photocurrent density–voltage ( $J-V$ ) characteristics and the corresponding external quantum efficiency (EQE) spectra for inverted P-DTG-TPD:PC<sub>71</sub>BM solar cells with 105 nm, 204 nm, and 258 nm-thick active layers. Figure 1 a shows that the short-circuit current density ( $J_{sc}$ ) increases with increasing active layer thickness due to enhanced light absorption, with the highest  $J_{sc}$  of 16.1 mA cm<sup>-2</sup> obtained for the device with an active layer thickness of 258 nm. The integrated current density from the EQE spectra, shown in Figure 1 b, is consistent with the measured  $J_{sc}$  with 5% deviation. The difference in the EQE spectra is due to optical interference effects between the incident light and light reflected from the Ag back electrode. For devices with thickness  $L \geq 200$  nm, the interference effects no longer affect the photocurrent density of the device and the active layer absorbs most of the incident light below 700 nm, resulting in EQEs above 70% from 400 nm to 700 nm.

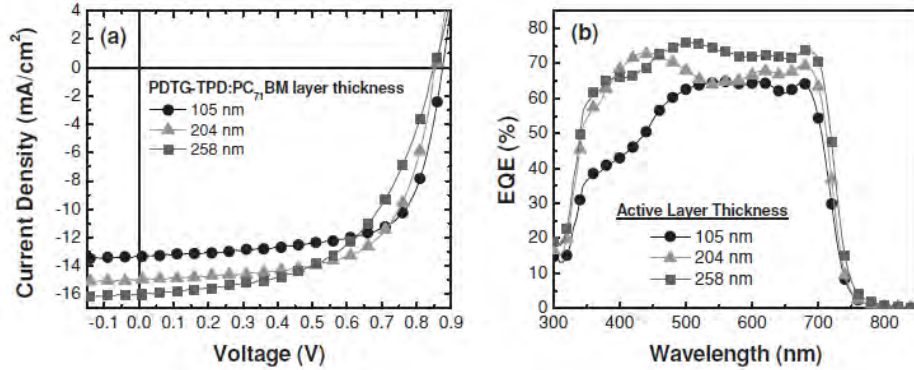


FIGURE 10 (A) CURRENT DENSITY VERSUS VOLTAGE CHARACTERISTICS FOR PDTG-TPD:PC 71 BM SOLAR CELLS WITH 105 NM, 204 NM, AND 258 NM-THICK ACTIVE LAYER. (B) CORRESPONDING EXTERNAL QUANTUM EFFICIENCY (EQE) SPECTRA FOR THE DEVICES.

**Table 1** summarizes the average solar cell parameters for the PDTG-TPD:PC<sub>71</sub>BM devices with an active layer thickness varying from 90 nm to 409 nm. The reduction in FF observed for PDTG-TPD solar cells with increasing active layer thickness is the major factor limiting the device performance. A power conversion efficiency (PCE) of 7.9% is obtained for the device with a 105 nm thick active layer, which is consistent with our

TABLE 1 AVERAGED SOLAR CELL PERFORMANCE FOR PDTG-TPD:PC 71 BM DEVICES WITH VARIOUS ACTIVE LAYER THICKNESS UNDER

Active Layer Thickness	$J_{sc}$ (mA cm <sup>-2</sup> )	$J_{sc}$ (EQE) (mA cm <sup>-2</sup> )	$V_{oc}$ (V)	FF (%)	PCE (%)
90 nm	12.5 +/- 0.1	12.3	0.88	68.5 +/- 0.1	7.5 +/- 0.1
105 nm	13.3 +/- 0.2	13.0	0.87	68.7 +/- 0.3	7.9 +/- 0.1
153 nm	13.5 +/- 0.4	13.5	0.86	68.1 +/- 0.3	8.0 +/- 0.2
204 nm	14.9 +/- 0.3	14.7	0.86	64.5 +/- 0.7	8.2 +/- 0.2
258 nm	16.1 +/- 0.2	16.0	0.85	54.1 +/- 0.9	7.4 +/- 0.1
409 nm	15.2 +/- 0.1	14.9	0.82	41.6 +/- 0.9	5.2 +/- 0.1

previous report. The efficiency remains constant for devices with  $L \leq 204$  nm, with an average PCE of 8.2% being obtained for devices with an active layer thickness of 204 nm. Above 200 nm, the FF reduction becomes significant, dropping from 69% in 105 nm film to 42% in 409 nm film.

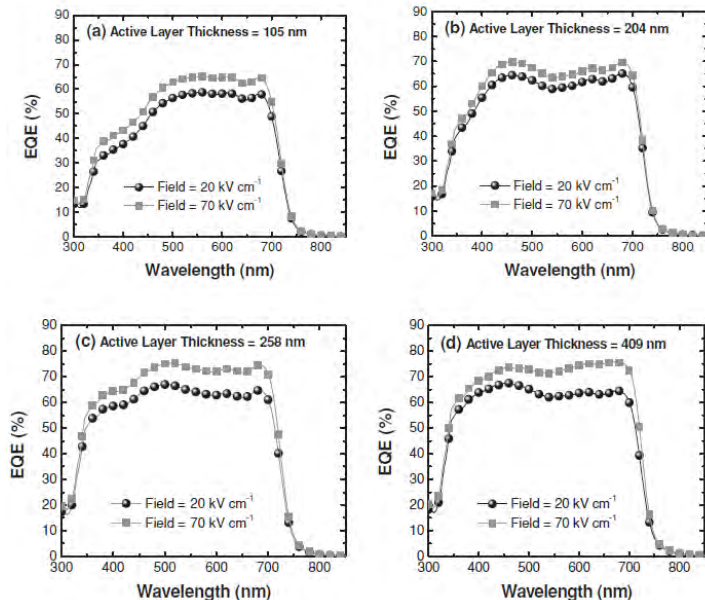


FIGURE 11 FIELD-DEPENDENT EQE SPECTRA FOR PDTG-TPD:PC 71 BM SOLAR CELLS WITH (A) 105 NM, (B) 204 NM, (C) 258 NM AND (D) 409 NM-THICK ACTIVE LAYER. THE EQE SPECTRA WERE MEASURED AT INTERNAL

To determine the root cause for the reduction in FF observed in the thick-film PDTG-TPD:PC<sub>71</sub>BM solar cells, the EQE spectra for the thin-film and thick-film devices were measured under different values of internal electric field. **Figure 2** shows the field-dependent EQE spectra for devices with 105 nm, 204 nm, 258 nm, and 409 nm-thick active layers, respectively. By measuring the EQE as a function of internal electric field ( $E$ ), approximated as  $E = (V_{oc} - V)/L$ , the effect of series resistance can be eliminated. For the device with an active layer thickness  $\leq 204$  nm, increasing the applied field from 20 kV cm<sup>-1</sup> to 70 kV



$\text{cm}^{-1}$  leads to a uniform enhancement in EQE across the entire spectral range. The increased applied field enhances the extraction of photogenerated charges equally across the EQE spectrum. Interestingly, for devices with  $L > 204$  nm, a stronger field dependent enhancement in EQE is observed in the spectral range from 500 to 750 nm when the applied field is increased from  $20 \text{ kV cm}^{-1}$  to  $70 \text{ kV cm}^{-1}$ . This wavelength range corresponds to the absorption spectrum for a pristine PDTG-TPD film. For devices with a thick active layer, the build-up of charges in PDTG-TPD:PC<sub>71</sub>BM will hinder charge collection and contribute to the FF reduction in thick solar cells.

To study the role space-charge accumulation plays in PDTG-TPD:PC<sub>71</sub>BM solar cells with a thick active layer, we employed the SCL photocurrent model to confirm that the electrostatic space-charge limit was reached in our thick devices. We compared the results for PDTG-TPD:PC<sub>71</sub>BM solar cells with similar devices based on P3HT:PC<sub>61</sub>BM, since P3HT solar cells provide a model system for studying space-charge effects. The effective photocurrent  $J_{ph}$ , normalized to the saturation photocurrent  $J_{sat} = qG_{max}L$ , was plotted on a double logarithmic scale against the effective voltage across the device, given by  $V_{eff} = V_0 - V$ . Here,  $V_0$  is defined as the voltage where  $J_{ph} = 0$  and is slightly larger than  $V_{oc}$ . This “corrected” photocurrent analysis is a widely used tool for analyzing recombination loss processes in organic solar cells. **Figure 3a** shows the results for the PDTG-TPD:PC<sub>71</sub>BM solar cells with 105 nm, 258 nm and 409 nm-thick active layer. For the device with a 105 nm thick active layer, two different voltage regimes can be observed. For  $V_{eff} < 0.30$  V,  $J_{ph}$  steadily increases with voltage due to the competition between diffusion and drift for photo-generated carrier transport at low field. For  $V_{eff} > 0.30$  V, the photocurrent saturates with increasing voltage. In this saturation regime, the internal field is strong enough to efficiently extract photogenerated carriers and the high field is responsible for the dissociation of  $e-h$  pairs. The voltage corresponding to the short circuit condition falls within the saturation regime, indicating that the high  $J_{sc}$  and FF obtained for this device is due to efficient charge collection by the internal electric field. For the device with a 105 nm active layer, space charge effects were not observed based on the data shown in Figure 3a. As the active layer thickness for PDTG-TPD cells increased above 200 nm, a square-root effective voltage dependence on  $J_{ph}$  is observed. This  $J_{ph} \propto V^{1/2}$  corresponds to the onset of space-charge limited photocurrent in thick PDTG-TPD cells assuming a  $J_{ph} \propto G^{3/4}$  dependence is also observed. The solid lines in Figure 3a correspond to  $J_{ph} \propto V^{1/2}$ . For the 409 nm-thick device, the  $J_{ph} \propto V^{1/2}$  regime extends to the short circuit condition, which correlates well with the reduction in  $J_{sc}$  and FF observed in this device. These results are in contrast with those found in **Figure 3b** for P3HT:PC<sub>61</sub>BM.



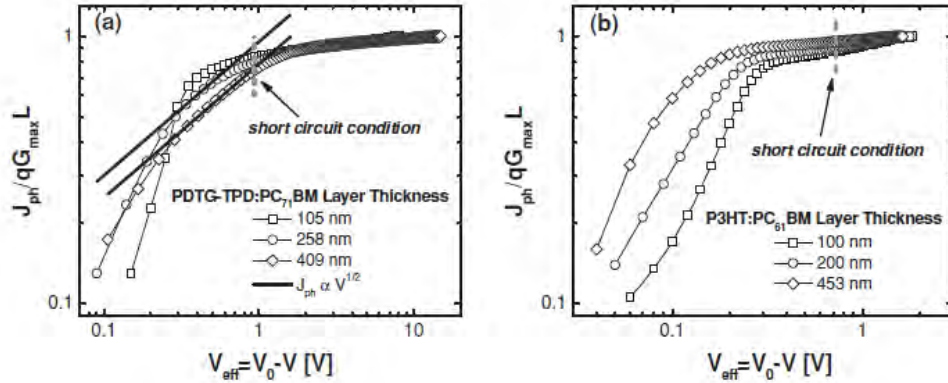


Figure 12 Effective photocurrent density ( $J_{ph}$ ) normalized by  $J_{sat} = qG_{max} L$  as a function of effective voltage ( $V_{eff}$ ) under  $100 \text{ mW cm}^{-2}$  illumination for (a) PDTG-TPD:PC<sub>71</sub>BM cells with 105 nm, 258 nm, and 409 nm-thick active layer, and (b) P3HT:PC<sub>61</sub>BM cells with 100 nm, 200 nm, and 453 nm-thick active layer. Dashed lines highlight the value of  $V_{eff}$  corresponding the short-circuit condition ( $V_{eff} = V_0$ ). The solid lines correspond to  $J_{ph} \propto V_{eff}^{1/2}$  fits of the photocurrent in the SCL regime for PDTG-TPD solar cells.

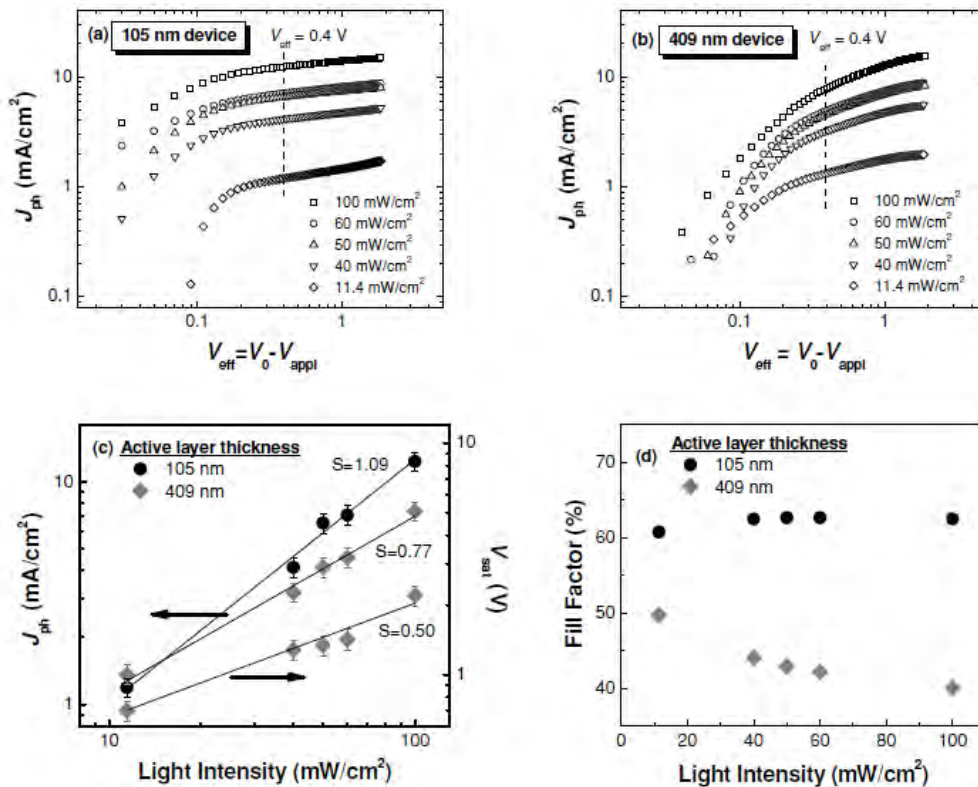


FIGURE 13 LIGHT INTENSITY DEPENDENT STUDY FOR PDTG-TPD:PC<sub>71</sub>BM SOLAR CELLS WITH THIN AND THICK ACTIVE LAYER.  $J_{ph} - V_{EFF}$  CURVES FOR THE (A) 105 NM-THICK AND (B) 409 NM-THICK DEVICES UNDER VARIOUS LIGHT INTENSITIES (FROM 11.4 TO 100  $\text{MW CM}^{-2}$ ). (C) EFFECTIVE PHOTOCURRENT DENSITY ( $J_{ph}$ ), SATURATION VOLTAGE ( $V_{SAT}$ ), AND (D) FILL FACTOR AS A FUNCTION OF INCIDENT LIGHT INTENSITY FOR THE SAME DEVICES. THE  $J_{ph} - P_0$  CURVES WERE MEASURED AT  $V_{EFF} = 0.4 \text{ V}$ .

The dependence of  $J_{ph}$  and FF on incident light intensity ( $P_0$ ) was plotted for the 105 nm and 409 nm-thick PDTG-TPD:PC<sub>71</sub>BM solar cells (see **Figure 4**). Neutral density filters were used to control the incident light intensity, which was varied from 11.4 to  $100 \text{ mW cm}^{-2}$ . The  $J_{ph} - P_0$  data for the thin and thick PDTG-TPD:PC<sub>71</sub>BM devices, shown in Figure 4c, was extracted from

the  $J_{ph} - V_{eff}$  curves shown in Figures 4a and b. For the solar cell with a 105 nm-thick active layer,  $J_{ph}$  showed a linear dependence on light intensity with the slope of the linear fit to the data equal to 1.09. In contrast, a slope of 0.77 is observed for the 409 nm-thick PDTG-TPD solar cell. The  $\sim 3/4$  power dependence of  $J_{ph}$  on the incident light intensity confirms the occurrence of SCL photocurrent in PDTG-TPD:PC<sub>71</sub>BM solar cells at low bias. The dependence of the saturation voltage ( $V_{sat}$ ) on incident light intensity provides further evidence, in which a slope of 0.50 is extracted from the  $V_{sat} - P_0$  data. To form a more clear physical picture, the light-intensity dependence of the FF was also analyzed and plotted in Figure 4d. The FF remained relatively constant with incident light intensity for the 105 nm-thick solar cell, which is expected since the device is not space-charge limited at  $P_0 = 100 \text{ mW cm}^{-2}$  and the thickness is sufficiently thin to ensure efficient charge extraction. For the 409 nm-thick PDTG-TPD solar cell, a 24% enhancement in FF was observed as the incident light intensity was decreased from  $100 \text{ mW cm}^{-2}$  to  $11.4 \text{ mW cm}^{-2}$ . By lowering  $P_0$  and, consequently, reducing the generation rate of charge carriers in the thick PDTG-TPD:PC<sub>71</sub>BM active layer, space-charge buildup was reduced. As a result, enhanced charge carrier collection and FF was observed in the solar cell. Despite this enhancement, the FF of the 409 nm-thick device at low light intensity does not reach the value obtained in the 105 nm device. This result indicates that the reduced photocurrent observed for thick-film devices could not be completely recovered despite lowering the incident light intensity. There is still some degree of limited charge collection occurring in thick-film PDTG-TPD:PC<sub>71</sub>BM solar cells.

To conclude, the loss mechanism in thick-film PDTG-TPD:PC<sub>71</sub>BM solar cells have been investigated. For polymer solar cells with an active layer thickness up to 200 nm, efficiencies in excess of 8.0% were obtained for devices under AM 1.5G illumination at  $100 \text{ mW cm}^{-2}$ . For  $L > 200 \text{ nm}$ , the SCL photocurrent regime is reached, leading to limited charge collection efficiency in the devices due to space-charge accumulation. The onset of space-charge accumulation also coincides with reductions in FF and hence power conversion efficiency in thick devices. These results indicate that although high efficiencies can be obtained in solar cells with low-bandgap conjugated donor-acceptor polymers, the high density of photogenerated charge carriers could severely limit the performance of solar cells with a thick active layer.

## **Florida Advanced Technological Education Center (FLATE)**

### ***Education - Technician Based Workforce***

### **(Progress Report)**

**PI:** Marilyn Barger

**Description:** FLATE (Florida Advanced Technological Education Center) will partner with FESC to develop statewide curriculum frameworks for technical A.S./A.A.S. degree programs supporting existing and new energy business sectors. FLATE will develop and have processed through the FLDOE the industry-validated student competencies of the frameworks. FLATE will also develop new courses required for each new program of study. Additionally FLATE will help state and community colleges implement the new frameworks in their institutions. To support the new curriculum, FLATE will work closely with the FESC Public Outreach and Industry Partnership programs to provide professional development opportunities for teachers and faculty to upgrade and update their knowledge base.

**Budget:** \$300,000.

**Universities:** FLATE/Hillsborough Community College

**FLATE External Collaborators:** Brevard Community College; Tallahassee Community College; Daytona State College; Central Florida Community College; Polk State College; Florida State College at Jacksonville; Valencia Community College; Palm Beach State College; School District Hillsborough County; Florida Department of Education – Division of Adult and Career Education; West Side Technical School; USF College of Engineering; Madison Area Technical College ATE project for Alternative Energy certifications; Milwaukee Area Technical College Energy Conservation and Advanced Manufacturing Center (ECAM); Florida Energy Workforce Consortium (FEWC); TECO; Progress Energy; ISTE (Ibero Science and Technology Education Consortium), Urbil GLBHI (Spain); TKNKA - Innovation Institute for Vocational Training (Spain); Center for Energy workforce Consortium (CEWD); UF Industrial Assessment Center; CREATE NSF Center for Alternative Energy; EST2 NSF ATE Grant project; DOE’s Office of Energy Efficiency & Renewable Energy; Gulf Coast State College; Palm Beach State College; University of South Florida’s College of Engineering; University of Miami; University of Alabama; Rutgers University; Energy Reduction Solution, SMC Corporation of America, Energy Conservation Group; Florida Solar Energy Consortium; Tampa Bay Regional Business Plan Energy Efficiency and Conservation Sub-Committee.

### **Progress Summary**

The development of the process for the Florida State College System to respond to FESC’s long term strategy to bring energy related technologies out of the Florida University System is well underway. Activities this year included identifying the current status of credit and non-credit energy related courses within the State College System. In addition, online curriculum related to Alternative Energy Systems has been developed. FLATE has the college contacts and process in place to respond to any FESC and/or regional economic development authority request to provide assistance to a designated State College because of a technician workforce development need as identified or triggered by a new or expanding energy related company’s operations in the State.

Since October 1, 2012 FLATE achieved several milestones. Together with the National Science Foundation-funded Energy Systems Technology Technicians (EST<sup>2</sup>) project team, FLATE has developed



Florida Energy Systems Consortium

a new Industrial Energy Efficiency specialization for the Engineering Technology (ET) Degree and associated College Credit Certificate.

Engineering Technicians are widespread in a variety of occupational areas, including electronics, applied technologies, manufacturing, and composites fabrication, to name a few. The new Industrial Energy Efficiency specialization track and college credit certificate (CCC) for the AS/AAS degree in Engineering Technology, comes at a time when green job sectors such as energy efficiency, are flourishing. Interest in reducing operating costs through energy efficiency maximization is growing significantly, both in Florida and throughout the nation. Collaboration with industry subject matter experts has allowed us to tailor the energy efficiency specialization curriculum and match training directly to industry needs.

Industry partners have indicated a need for energy efficiency measures to help their bottom line, and as a result the new specialization/CCC is designed to help incumbent technicians in manufacturing or industrial occupations find ways to save money through efficiency in their industrial setting, or prepare students to become energy managers or auditors. Upon completion of the program, students will be armed with the knowledge and skills necessary to implement energy efficiency strategies in industrial processes and systems, and as a result impact the bottom line. It will help the student prepare to become a SEP-Superior Energy Performance Certified Systems Practitioner and a CEM Certified Energy Manager. The program will also help train workers who will assist a company in achieving the ISO 50001 standards related to energy management, as well as ISO 14001:2004 to assure a company's stakeholders that measures are being taken to improve their environmental impact.

The EST<sup>2</sup> team (comprising individuals from Brevard Community College, Florida State College at Jacksonville, Tallahassee Community College and Hillsborough Community College), submitted the framework to the Florida Department of Education at the beginning of 2013 and colleges will be able to implement it in the 2013-2014 academic year.

Program Title: Industrial Energy Efficiency Specialist (CCC)  
Career Cluster: Manufacturing

CIP Number	TBD
Program Type	College Credit Certificate (CCC)

Program Length 21 Credit Hours (Primary), 24 Credit Hours (Secondary)

This certificate program is part of the Engineering Technology AS/AAS degree program (1615000001/0615000001).

FLATE and FESC coordinated a second highly successful energy workshop (the last one was held in September 2011 in Gainesville), for high school and college educators, as well as industry partners, hosted by the Florida Solar Energy Center (FSEC) in Cocoa, FL on January 25, 2013. Forty attendees attended a wide variety of presentations, went on a tour of the amazing FSEC facilities and participated in a Professional Development activity focused on solar energy applications. Feedback received was overwhelmingly positive.

FLATE and FESC coordinated an Advisory Working Group Meeting in Orlando, FL on February 28, to develop a curriculum plan for the Industrial Energy Efficiency Technician (IET) Specialization. Sixteen members from academia and industry worked on the following focus statement for the workshop, "An industrial energy efficiency technician implements energy efficiency strategies in industrial processes and systems in order to improve an organization's bottom line and reduce environmental impacts."



As a result of the meeting, a comprehensive list of IEET Resources was compiled and classes were identified as well as their associated learning outcomes.

Finally, FLATE regularly updates / presents information about energy curriculum and training issues at the statewide Florida Engineering Technology Forum that meets twice per year at various colleges across the state. Many of these schools are looking to add “energy” curriculum and/or programs and are requesting guidance on what industry is asking for across the state and what and how other colleges are implementing credit programs. The goal of these activities is to keep colleges working together and sharing curriculum rather than develop independent programs not properly aligned to statewide frameworks. The ET Forum most recently met April 4 - 5 in Clearwater at St. Petersburg College.

**Activities for the 2012-2013 year are listed below.**

- Presented at the Florida Association of Science Teachers Conference in October, 2012 with Mark Dick (Tallahassee Community College), “Energy Camps that are Energizing”, highlighting the Teacher Energy Workshops and Energy Summer Camps for students offered over the summer by all EST 2 partners.
- Attended the Florida Energy Workforce Consortium Meeting in November 2012 and March 2013.
- Presented “Industrial Energy Efficiency Competencies for Associate Degree Programs”, at the Interstate Renewable Energy Council (IREC) Clean Energy Workshop in Albany, NY, November, 2012.
- Attended the Manufacturers Association of Florida Summit in December 2012 and surveyed 40 manufacturers about the need for energy efficiency trained technicians. The overwhelming majority of manufacturing members who completed the survey strongly supported the new IEET CCC since manufacturers need solutions to their high cost associated with energy consumption. A focus group meeting was held in Orlando, in February 2013 with industry, university faculty, tech center faculty and state college personnel/faculty. The focus group meeting was a scaled down, Designing a Curriculum (DACUM) that produced potential courses and course content for the proposed IEET program. The course creation validated the IEET program framework content that went to the FL Department of Education for approval at the beginning of this year, and will be implemented in the 2013-2014 academic year.
- Coordinated a second Community College Energy workshop for 40 attendees at the Florida Solar Energy Center (FSEC) in Cocoa, January 25, 2013.
- Was instrumental in the selection of Hillsborough Community College as a winner of the (Sustainability Education and Economic Development) Green Genome Award which recognizes exemplary community colleges nationwide that have taken a strategic leadership role in sustainability and green economic and workforce development.
- Attended and was part of an Energy Efficiency and Conservation Panel at 2013 Beyond Sustainability 37<sup>th</sup> Annual Conference at Hillsborough Community College, Plant City in February.
- Participated in, “An Energy Literate Citizenry from K-to-Gray: A Webcast on the Department of Energy’s Energy Literacy Initiative”, in March.
- FLATE hosted the Engineering Technology (ET) Forum in St. Petersburg on in April. (Energy Efficiency Specialization was presented).
- Planning underway to host a third summer energy program for under-represented middle school students, to be held July 8 – 11 at HCC’s SouthShore Campus in Ruskin, FL in conjunction with the EST2 grant partners (BCC, TCC and FSCJ).





Florida Energy Systems Consortium

Funds leveraged/new partnerships created: FLATE has leveraged its NSF and FESC resources to help Brevard Community College to apply for and be awarded a very competitive NSF grant, \$ 500,000, implement two energy related specialization within the A.S. Engineering Technology Degree. In addition, FLATE was able to secure a \$ 1 00,000 award from NSF to develop a faculty/student interchange that will allow Florida to benefit from the well advanced energy related technology education practices at technology colleges in Spain.





## **FESC OUTREACH PROGRAM**

### ***Educational Outreach Programs***

### **(Final Report)**

**PI:** Dr. Pierce Jones, Director, Program for Resource Efficient Communities (PREC)

#### **Outreach Team Members:**

- Dr. Kathleen C. Ruppert
- Hal S. Knowles III
- Nicholas Taylor
- Dr. Barbra Larson
- Craig Miller
- Ms. M. Jennison Kipp Searcy

#### **Executive Summary**

The goal of the program is to develop educational outreach programs and materials designed to deliver practical, applicable information and knowledge on energy-related topics to the general public as well as targeted to specific audiences such as builders, planners, engineers, architects, small businesses, local governments, and utilities through the Cooperative Extension Service and others. By focusing educational programming on climate and efficient use of energy and water, the program aims to provide the knowledge needed by building and energy professionals, local governments, and the general public, to significantly reduce greenhouse gas emissions in Florida.

#### **Sustainable Floridians<sup>SM</sup> Program**

The outreach team developed the Sustainable Floridians<sup>SM</sup> Program during the reporting period. The program details and progress are given below.

Sustainable Floridians<sup>SM</sup> is a statewide educational program that was piloted in 2010 and 2011 to teach Floridians how to improve their economic, environmental and social sustainability and that of the communities in which they reside. The program was developed at the University of Florida's (UF) Department of Family, Youth and Community Sciences in collaboration with the UF/IFAS Program for Resource Efficient Communities, the UF Office of Sustainability and UF/Extension Faculty in seven counties.

The program's curriculum is both educational and action-oriented, and is directed at citizens who enroll in the class through a County Extension Office participating in the program.

#### **Goals and Objectives:**

The Sustainable Floridians<sup>SM</sup> course encourages individuals and communities to become more resilient at the local community level. Beyond the objective of developing an educated citizenry, the goals include:

- Increasing participants' knowledge about sustainability issues at the global, state and local levels,
- Providing information that identifies Florida-specific actions for conserving energy and water,
- Motivating participants to implement conservation and efficiency actions that save resources and money, and



Florida Energy Systems Consortium

- Creating opportunities for community level leadership in sustainability education in a variety of settings from offices to community and neighborhood organizations

Participants meet with the program facilitator for six to seven weekly sessions. The classes include topics such as Why Should I Care?; Principles of Sustainability; Energy; Water; Transportation and Land Use; Food Systems; Consumerism; Community Leadership, etc. The course is very participatory and a variety of teaching methodologies are used including weekly handouts, multi-media presentations, supplemental readings and a textbook that allow participants to examine the material individually and then collectively. The course engages participants in group discussion, group and individual reflection, and personal action.

One example of a successful program is Pinellas County. Pinellas County Extension offered the program as part of the pilot initiative and continues to offer it as part of its sustainability curriculum. Pinellas County, one of 35 coastal counties in Florida, borders Tampa Bay and the Gulf of Mexico, has a population of 916,000 residents, and is considered the 6th most densely populated county in the state. Sustainability is a critical issue for a 97% “built-out” county with 25 different local governments. Although a challenge, balancing resource use with human and economic needs is critical to a successful and thriving local economy. Achieving this goal is possible with a motivated, engaged and educated citizenry. Since the start of the program, Pinellas trained 66 participants who have donated over 1,800 volunteer hours, a value of \$33,588 (using \$18.66 per hour as provided by Extension).

In Leon County, graduates are serving as facilitators for local EcoTeams, which are discussion circles organized within neighborhoods, faith organizations and other groups, under the sponsorship of Sustainable Tallahassee, a partnership umbrella NGO.

In addition, all participants are encouraged to track their monthly energy, water and vehicle miles travelled, and use consumption logs to develop a personal sustainability plan.

The Sustainable Floridians<sup>SM</sup> program has proven instrumental in filling the need for sustainability education within the community-at-large. The participatory course structure allows trainees to explore a range of educational material that will encourage sustainable practices and improve the economic, environmental and social conditions of their communities.

The County Extension offices are well positioned to provide education at the local level and possess the necessary infrastructure to support sustainability education at the community level.

The Sustainable Floridians<sup>SM</sup> program is now active in four counties...Leon, Osceola, Pinellas, and Sarasota. Marion County had an active program but the coordinator recently moved to take a position in Mississippi. Several other counties are contemplating beginning the program in the near future. While some counties train the participants to fulfill volunteer roles, other counties see the program as solely an educational program that they believe will have a ripple effect of educating others.

The program, up until recently, had no statewide coordination following completion of the pilot program. Now, with the assistance of UF’s Office of Sustainability, UF’s Program for Resource Efficient Communities through the Florida Cooperative Extension Service is working with county Extension faculty to develop curriculum review teams, an advisory committee, and all of the actions and activities needed to operate a statewide program. While in the midst of updating existing modules, along with creating new materials and determining efficiencies of scale, the program is continuing to gain statewide interest as indicated by the 16 counties represented at a recent in-service training.



# A Critique of Alternative Power Generation for Florida by Mechanical and Solar Means

## AUTHORS

**Robert H. Weisberg**  
**Yonggang Liu**  
**Clifford R. Merz**  
 College of Marine Science,  
 University of South Florida

**Jyotika I. Virmani**  
 Florida Institute of Oceanography

**Lianyuan Zheng**  
 College of Marine Science,  
 University of South Florida

## Introduction

When compared with other locales, the potential for electrical power generation by alternative energy sources may seem to be relatively good for Florida, a subtropical peninsula, which is nearly surrounded by water and bathed in sunlight. Herein, we critically assess this potential using observations of winds, incoming short-wave radiation, ocean currents and waves, supplemented by other data and model simulations. The Ocean Circulation Group at the College of Marine Science, University of South Florida (OCG-CMS-USF), through the CMS Coastal Ocean Monitoring and Prediction System (COMPS), began collecting such serial observations on the West Florida Continental Shelf (WFS) in 1998. We analyze these data to determine the energy fluxes (energy per unit area per unit time) that are available through natural processes, then transform these energy fluxes into practical power-generation time series based on either commercial literature or physically reasonable assumptions, and

## ABSTRACT

Using observations of surface winds, solar radiation, ocean currents and waves collected by the University of South Florida, Coastal Ocean Monitoring and Prediction System (COMPS), augmented by other data and numerical model simulations, we address the potential for electrical power generation for Florida by harnessing the natural energy sources of wind and solar, along with ocean currents and waves. We begin by identifying what nature offers. For wind and solar, we use specifications from existing, commercially available devices to convert nature's bounty to power-generation estimates. In the absence of mature, commercially available devices for ocean currents and waves, we draw upon physical principles to arrive at power-generation estimates for these potential sources. On the basis of what nature offers and what machinery may be capable of producing, we then make reasonable extrapolations on what these estimations may mean in a practical sense for supplying energy to society. Power generation from these naturally occurring, alternative energy sources, particularly wind and solar, may provide a means for supplementing power generation by conventional fuels but does not provide a replacement for conventional fuels. **Keywords:** alternative power generation, ocean observations, windmills, watermills, waves, solar

then compare the results with consumptive metrics. The purpose is to demystify the concept of alternative power generation by mechanical and solar means and to place realistic expectations on what may be achievable for the state of Florida under typical, natural conditions. While our work is specific to Florida (and primarily west central Florida), the findings, with some modifications, are expected to also apply elsewhere.

The article is organized as follows. Each of the subsequent four sections deals with power-generation potential by winds, ocean currents, ocean waves, and incident solar radiation, respectively. For each medium, we use either WFS observations collected by the COMPS program, or model simulations, along with specifications from commercially advertised devices, or

reasonable assumptions, for converting the natural energy fluxes to power generation. Given nature's bounty and how much of this may be converted to electrical power, the Discussion section then presents these findings relative to consumptive metrics, such as the requirement for powering a household and the economics of doing this. Not included, however, are any discussions on other complicating matters such as electrical transmission, storage, or daily to seasonal variations in peak or base loads that must be accommodated on a utility scale. Conclusions follow in the last section.

## Wind The Data

An offshore array of WFS COMPS moorings (Figure 1) was initiated in

## FIGURE 1

Map of the West Florida Continental Shelf COMPS stations. Observations from mooring C10, located approximately 25 nm offshore from Sarasota, FL, are used herein.



1998. In addition to measurements of velocity, temperature, and salinity over the water column, as many as five surface moorings also collected meteorological data. Water velocities (currents) were measured using RD Instruments (now Teledyne) acoustic Doppler current profilers (ADCP), and meteorological variables were measured using either Coastal Environmental Systems (CES) Weatherpaks or Woods Hole Oceanographic Institution (WHOI)-designed Improved METeorological/Air-Sea Interaction METeorological (IMET/ASIMET) sensor suites. The surface moorings all measured air and sea surface temperatures, relative humidity, barometric pressure, and wind speed and direction. The IMET/ASIMET system and one of the Weatherpaks also measured downward long-wave and short-wave radiation. The IMET/ASIMET sampling consisted of 12; 5-s intervals formed into a 1-min average every 20 min. The Weatherpak data were collected every second for 15 min and averaged to provide 15-min samples. After quality control, these (either 15- or 20-min) samples were then

formed into hourly averages for further analysis. A review of these observations is provided by Weisberg et al. (2009).

Wind speed and direction were measured using RM Young 5103 Wind Monitor sensors at either 2.8 or 3.2 m above the sea surface on the IMET/ASIMET or the Weatherpak buoys, respectively. In either configuration, these observations were adjusted to a standard 10 m height above sea level using a log boundary layer scaling under neutral stability (e.g., Large & Pond, 1981). For the purpose of applying such buoy wind observations to large-scale commercial wind turbines, a further adjustment was needed to account for the turbine hubs being located some 80 to 100 m above the sea surface. Using a 100-m hub height, we estimated the wind speed there ( $U_{100}$ ) from the wind speed at the standard 10-m level ( $U_{10}$ ) by

$$U_{100} = U_{10} \frac{\log(z/z_0)}{\log(10/z_0)} \quad (1)$$

where  $z_0$  is the surface roughness, which, for open water exposure, was

taken to be 0.015 m. Recognizing that such log layer scaling (yielding an amplification factor of 1.35) is merely an approximation, we acquired National Centers for Environmental Prediction (NCEP) North American Mesoscale (NAM) modeled wind results as a check. Downloaded from <http://nomads.nccdc.noaa.gov/data/naman/> for six sites along a shore-normal line intersecting Sarasota, FL, for the period 1/1/12 to 4/12/12 (such multiple level results are not available for earlier times), a linear regression between winds modeled at 10 and 80 m heights (the lowest levels available) for the offshore open water exposure sites yielded a coefficient of 1.16, less than the log layer scaling result. Thus, the use of 1.35 as a conversion factor from 10 to 100 m winds is offered as a conservative estimate, overestimating, versus underestimating the winds aloft, on average.

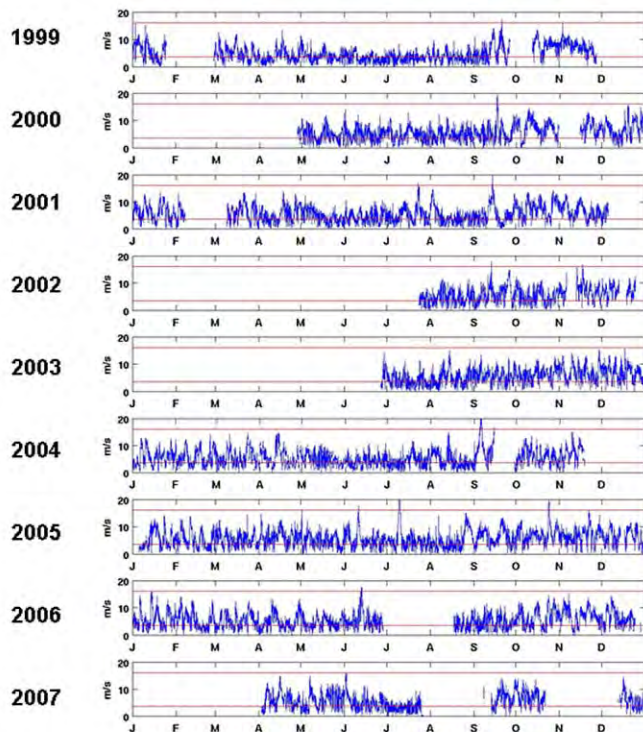
On the basis of these (hourly averaged) wind observations scaled to a hub height of 100 m, and using mooring C10, located about 25 nm offshore from Sarasota, FL, Figure 2 shows what was available for wind power generation at this site over the 8-year interval, from 1999 to 2007. The values range from zero to around  $20 \text{ m s}^{-1}$ , but with the higher end occurring only on rare occasions during the passage of tropical storms.

Whereas our analysis is limited to a single point off the west central Florida coast, these winds are representative of winds elsewhere in Florida with some caveats. On both long-term and seasonal averages, the winds tend to increase from north to south by virtue of the trade winds' meridional structure and Florida peninsular land effects (e.g., Weisberg et al., 2009; Liu & Weisberg, 2005), which also results



## FIGURE 2

Hourly averaged winds scaled to 100-m hub height using C10 observations from 1999 (top) through 2007 (bottom). The lower and upper red lines indicate the turbine cut-in value of  $3.5 \text{ m s}^{-1}$  and the rated power-generation wind speed of  $14 \text{ m s}^{-1}$ , respectively.



in the trade winds being a little stronger on the east coast. For synoptic scale weather events, the entire state of Florida is similarly affected. On the diurnal time scale, the east coast sea breeze tends to be more regular than that on the west coast.

### Converting Wind Speed to Electrical Power-Generation Potential

Commercially available wind turbines are discussed with respect to their nameplate-rated power-generation capacity. This can be misleading because the actual power output depends on wind speed. As a representative example we consider a General Electric (GE) 3.6 MW Offshore Series Wind Turbine, with specifications that are available in a brochure, which may be downloaded from the manu-

facturer's Internet site. From the wind load-power curve, we see that the turbine does not begin to produce electrical power until the wind speed exceeds  $3.5 \text{ m s}^{-1}$  (the cut-in wind speed). Power generation then increases with increasing wind speed, reaching the nameplate-rated capacity (3.6 MW) at a wind speed of  $14 \text{ m s}^{-1}$  (the rated wind speed), and the device ceases power generation and shuts down when the wind speed exceeds  $27 \text{ m s}^{-1}$  (the cut-out wind speed). The lower and upper horizontal lines on Figure 2 represent the cut-in and the nameplate-rated capacities for the GE 3.6 MW turbine, respectively. From 8 years of WFS data, we see that the winds at 100-m hub height fail to drive the turbine some 20% of the time and that rarely do the winds reach the nameplate rated capacity.

To determine what the power output may be when the turbine is running, we fitted a polynomial to the power curve provided by the brochure, and we used this to convert wind speed to power output for speeds between the cut-in and rated capacity values. For wind speeds between  $14$  and  $27 \text{ m s}^{-1}$ , the output was held constant at 3.6 MW (Figure 3). The results, further averaged to provide daily values, are shown in Figure 4, from which several points are clear. First, the nameplate-rated capacity is rarely achieved. Second there are many days (excluding the larger interval data gaps) when the cut-in speed of  $3.5 \text{ m s}^{-1}$  is not exceeded, and hence no power is generated. Third, when looking at the climatological monthly mean time series (the lowest panel) obtained by averaging all Januarys, all Februarys, etc., we see that minimum and maximum power generation occurs in summer and fall months, respectively. The monthly mean minimum is about 0.6 MW, the monthly mean maximum is about 1.8 MW, and the grand average across all years and months is about 1 MW. The minimum in summer months is troublesome for Florida because that is when the demand for air conditioning is the largest.

### Ocean Currents The Physics

Unlike windmills, where commercial maturity provides known power-generation potential, watermills driven by ocean currents remain in development. Estimating the potential for power generation by ocean currents requires that we begin from first principles. Available power,  $P$ , for potential extraction from ocean currents is the kinetic energy flux,  $\frac{1}{2}\rho V^3$ , times the area,  $A$ , of the device used for extracting

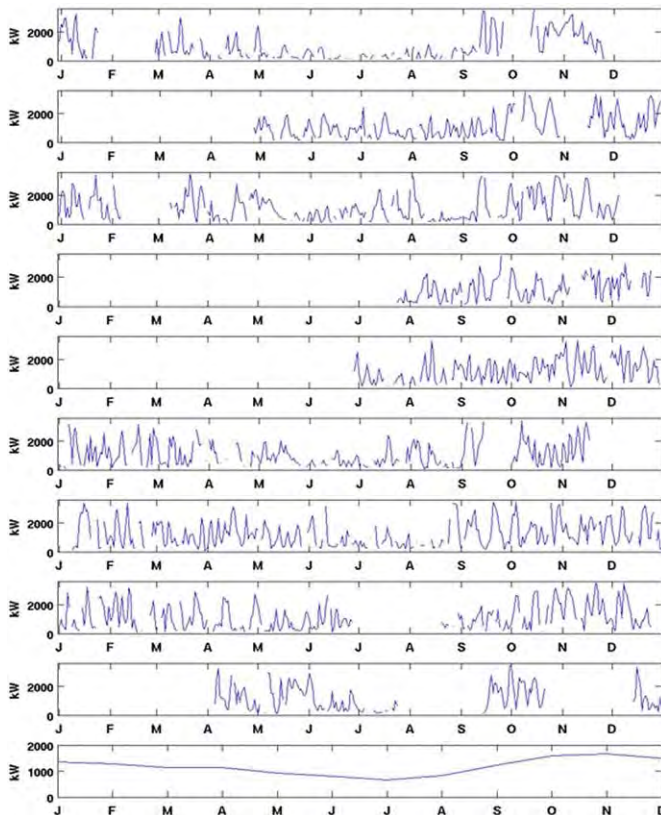
### FIGURE 3

A polynomial fit to a power curve provided for a GE 3.6 MW wind turbine (see ge\_36\_brochure. PDF available at <http://www.gepower.com>). The power curve gives the machine output in kW as a function of wind speed in  $\text{m s}^{-1}$ .



### FIGURE 4

Daily-averaged power and climatology of power using C10 wind speed observations scaled to 100 m hub height, from 1999 (top) through 2007 (bottom).



this flux, or  $P = \frac{1}{2}\rho V^3 A$ , where the units for  $P$  are watts (W). Watermills, like windmills, are subject to the same hydrodynamic limitations embodied in Betz's law (Betz, 1920), which states that the maximum power that may be extracted is 59% of the kinetic energy flux offered by nature. Additional losses come from the efficiency of the device itself, such that the expected power-generation potential for either a windmill or a watermill is in the approximate range of 40-50%.

Watermills, like windmills, are also expected to have a cut-in speed threshold below which they will not function. In other words, a baseline torque is necessary to drive an electrical generator. Given that torque equals force times distance, it is proportional to the pressure on a turbine blade times both the area and the length of the blade. A dimensional analysis, making use of Bernoulli's theorem, suggests that the cut-in speed may scale as  $S_w = S_a \sqrt{\rho_a / \rho_w} \frac{L_a}{L_w}$ , where  $S$  denotes the cut-in speed,  $\rho$  the density and  $L$  the length, and the subscripts  $a$  and  $w$  denote air and water, respectively. Using the cut-in speed for the GE 3.6 MW turbine and its length scale and assuming that a watermill may have a length scale about an order of magnitude smaller than the windmill, we arrive at a cut-in speed estimate of around  $1 \text{ m s}^{-1}$  for the watermill. Granted, this is a very crude estimate, but what it does suggest, even if off by a factor of two to four, is that typical coastal ocean current speeds on the continental shelf (away from tidal inlets), which are of order  $0.2$  to  $0.5 \text{ m s}^{-1}$  (e.g., Weisberg et al, 2009; Liu & Weisberg, 2005), are too small to drive watermills. Nevertheless, Florida does have a strong western boundary current seaward of its continental



shelf, for which we can examine the potential utility of power generation by watermills. For the west coast of Florida this western boundary current is the Gulf of Mexico Loop Current, which feeds into the Gulf Stream on the east coast of Florida. Being that the Gulf Stream is tightly constrained to flow between Florida and the Bahamas, this is the most practical place for considering power generation by watermills.

### Application to the Gulf Stream

The Gulf Stream, as it flows through the channel between Florida and the Bahamas, is highly baroclinic, with maximum speeds generally located at the surface toward the western side of the channel (see Figure 5, after Leaman et al., 1987). Speeds near the surface, and approximately within a baroclinic Rossby radius of deformation from the Florida side, are as high as  $2 \text{ m s}^{-1}$  (4 kts), diminishing rapidly with depth to about  $1 \text{ m s}^{-1}$  at 300 m depth and then to less than  $0.5 \text{ m s}^{-1}$  below 500 m depth. The total volume flux through the Florida Straits has long been recognized to be around  $30 \times 10^6 \text{ m}^3 \text{ s}^{-1}$  (or Sverdrups) (e.g.,

Stommel, 1965; Niiler & Richardson, 1973; Leaman et al., 1987).

For our purposes, we use velocity time series simulated by a numerical circulation model to estimate the power-generation potential for the Gulf Stream. The model chosen is the global Hybrid Coordinate Ocean Model (HYCOM) run by the U.S. Navy Research Laboratory and the HYCOM consortium (e.g., Chassignet et al., 2007, 2009). Figures 6 and 7 show volume and kinetic energy transports, respectively, for transects at the latitudes of Miami, FL, and Palm Beach, FL. In each of these figures, the transports were calculated over three different depth intervals, 0 to 50 m, 50 to

300 m, and 300 m to the bottom, plus the total transports across the entire cross sections. The first of these figures provides a check on the HYCOM simulation. From it, we see that the total transports properly represent the observations to within reasonable bounds on natural variability and measurement error. This provides justification for using these model simulation results to discuss the kinetic energy flux and how these integrate to provide estimates on power-generation potential.

Two practical considerations come to play. First, with sea state under northerly winds being very large at times across the Florida Straits, it would be difficult, if not impossible,

### FIGURE 5

A Gulf Stream cross section for the north component of velocity sampled at  $27^\circ\text{N}$  (from Leaman et al., 1987).

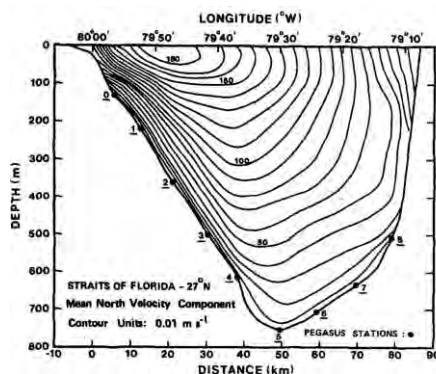


### FIGURE 6

Gulf Stream volume transport across two sections between Florida and the Bahamas at the latitudes of Miami, FL, and Palm Beach, FL, calculated for the calendar year 2008 using a Global HYCOM simulation. Transports are shown for three different depth intervals, plus the total transport across the entire cross sections. The dashed lines on the bottom panel provide the year-long averages. (Color versions of figures available online at: <http://www.ingentaconnect.com/content/mts/mts/2012/00000046/00000005>.)

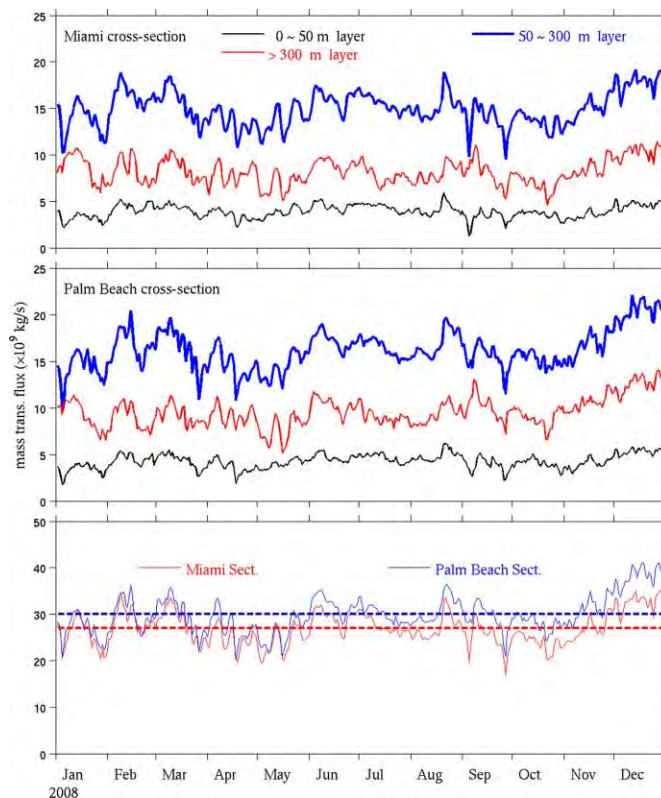
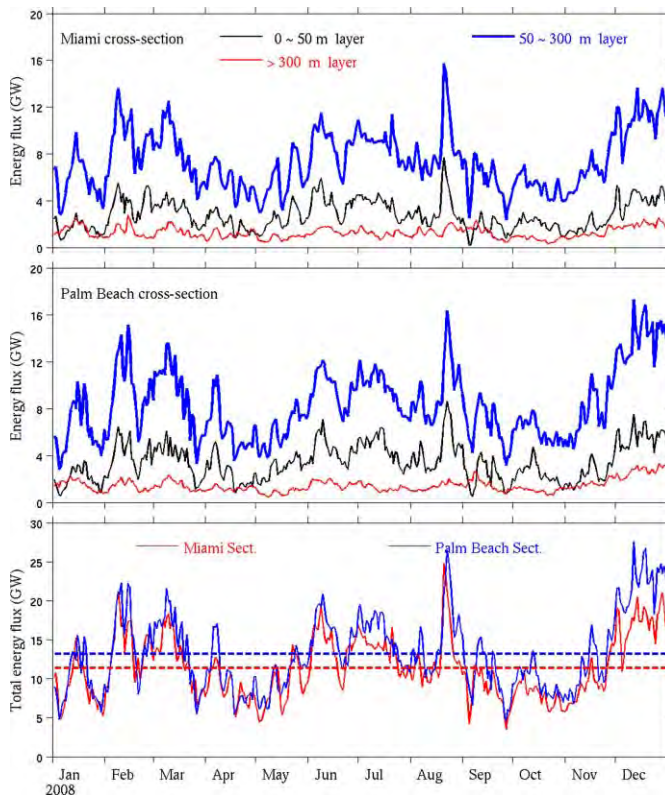


## FIGURE 7

Gulf Stream kinetic energy transport across two sections between Florida and the Bahamas at the latitudes of Miami, FL, and Palm Beach, FL, calculated for the calendar year 2008 using a global HYCOM simulation. Transports are shown for three different depth intervals, plus the total transport across the entire cross sections. The dashed lines on the bottom panel provide the year-long averages.



to operate turbines within the upper 50 m of the water column. For instance, the wavelength for a deep-water wave of 8 s period is 101 m; hence, particle speeds for waves of longer period would impact the flow field at 50-m depth. Second, with current speeds generally less than  $0.5 \text{ m s}^{-1}$  below 300 m there is likely little potential for energy generation by watermills below that depth. Given these practical considerations, it is reasonable to limit our attention to a depth interval of 50-300 m.

For the depth range of 50-300 m, Figure 7 shows that the annual mean power that may potentially be tapped by watermills is about 7.4 and 8.3 GW at the Miami and Palm Beach trans-

ects, respectively. These potential values are less than the corresponding total Gulf Stream cross-sectional annual mean power estimates (surface to bottom) of 11.4 and 13.2 GW, respectively. The approximate 2.7 and 4.3 GW of the upper 50 m, respectively, are not available, nor are the approximate 1.3 and 1.4 GW below 300-m depth, respectively, for the practical reasons just provided. Moreover, the application of Betz's law, plus additional mechanical losses reduces the power potential by at least 50% to about 3.7 and 4.1 GW for the Miami and Palm Beach transects, respectively. Further recognizing the impossibility of filling the entire cross section depth range with turbines re-

duces these numbers by at least another order of magnitude. The end results are the more realistic potentials of 370 and 410 MW for these Miami and Palm Beach sections, respectively. But even these numbers are likely to be overestimates because any watermill will have a water load-power curve just like a windmill (e.g., Figure 3) so its power output will be further reduced from that potentially provided by nature. Given what an actual watermill cut-in speed and water load-power curve may be, it is probably reasonable to reduce the above by a factor of two and settle on about 200 MW as a potential estimate. This would be equivalent to what may be obtained from about 200 (GE 3.6 MW) windmills if operated under West Florida wind conditions (Converting Wind Speed to Electrical Power Generation Potential).

Because windmills installed on either land or offshore and watermills installed within the Gulf Stream (the most powerful of the ocean currents adjacent to the United States) tend to have similar promise for power generation, it is useful to consider two additional factors. The first is a matter of scale. Being that windmills and watermills rely on products of fluid density times fluid velocity cubed times area ( $\rho V^3 A$ ), it is apparent that (with air being approximately a thousand times less dense than water while air velocity is about ten times faster than water) the area necessary to generate comparable amounts of power in air and water are the same. This begs the question: if the size of the machinery must be the same in air and water, why would we choose to work in a fluid medium (water) that is technologically so much more challenging than air? The second consideration is even more daunting. Windmills deployed in air operate within the lower



100 m of the atmosphere or in the lower part of the frictional boundary layer, which is driven by and continually replenished by the geostrophic interior that extends to the tropopause, some 10 km aloft. Watermills, in contrast, operating across a major portion of the water column, are in the geostrophic interior itself and hence, unlike windmills, have no natural means for replenishing the energy that they may extract. It is for this reason that windmill farms may have closely spaced units with additional windmills even distributed downwind from one another. Watermills, in contrast, cannot share this deployment strategy. Once power is removed from a cross section, it cannot be readily replenished. For these two reasons, even in the swiftest of currents, like the Gulf Stream, the notion of power generation by watermills tapping the kinetic energy flux seems very limited when compared with what may be achieved by windmills.

## Ocean Waves

### The Physics

Waves, like currents, also possess an energy flux that may be tapped by mechanical devices. The available power,  $P_W$ , for potential extraction from ocean gravity waves is the total mechanical energy flux per unit wave crest width,  $\frac{1}{2}\rho g a^2 C_G$ , times the crest width length,  $L$ , of the device used for extracting this flux, or  $P_W = \frac{1}{2}\rho g a^2 C_G L$ , where  $g$  is the acceleration of gravity,  $a$  is the wave amplitude,  $C_G$  is the group velocity, and the units for  $P_W$  are watts. An alternative expression for  $P_W$ , based on significant wave height and application of the deep water dispersion relation, is  $P_W = \frac{1}{2}H_s^2 TL$ , where  $T$  is the wave period and significant wave height  $H_s$ ,

is defined as the average of the highest third of the waves.

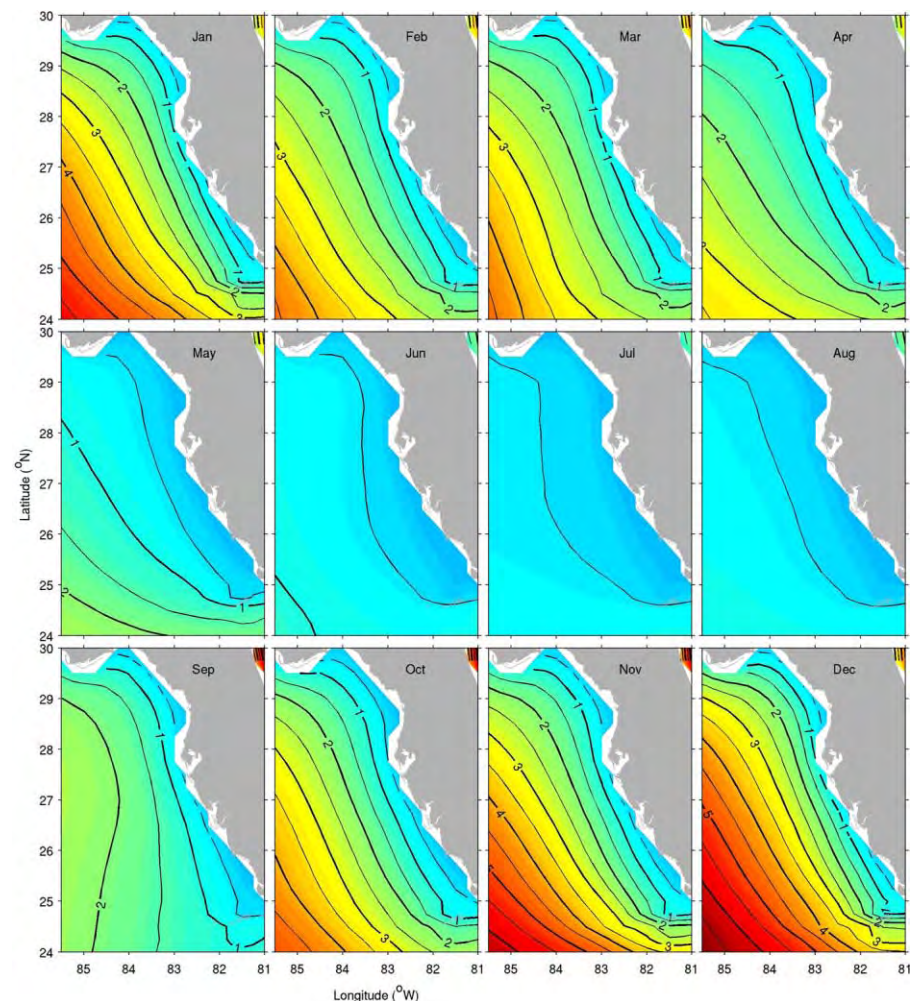
### Application to the WFS

Several point measurements of surface gravity waves are available for the WFS, either from COMPS observations or a NOAA NWS weather buoy. As it is more instructive to look at the entire field of waves and how this varies throughout the year, we opted to base our estimates on numerical model simulations, of which there are several. The longest of these is

from the NOAA application of the WaveWatch III model, e.g., Tolman (1991, 1999, 2010). Figure 8 shows a monthly mean wave energy flux per unit crest width climatology for the WFS with contour units of  $\text{kW m}^{-1}$  calculated from an 8-year analysis of WaveWatch III model results inclusive of 1999 to 2007. A robust annual cycle is seen with minimum wave energy in summer and maximum wave energy in winter, similar to that of the significant wave height measured at NDBC Buoy 42036 (Liu et al., 2010). This finding

**FIGURE 8**

Monthly mean surface gravity wave energy flux per unit crest width calculated for the WFS using the WaveWatch III reanalysis from 1999 to 2007. The contour units are  $\text{kW m}^{-1}$ , and each of the monthly climatologies is calculated by averaging all similar months, i.e., all Januarys, all Februarys, etc.



is consistent with the prevailing wind directions for the WFS varying from southeasterly in summer to northeasterly in winter (e.g., Liu & Weisberg, 2005). With low wave energy, the WFS is not very promising for alternative power generation by tapping the energy flux of surface gravity waves, except perhaps for running low power instruments *in situ*.

The east coast of Florida does have a larger wave climate, especially north of the Bahamas where the entire fetch of the north Atlantic comes to play. But even there the energy flux per unit crest width remains small compared with other higher energy coastlines worldwide (Figure 9), where tens to even a hundred  $\text{kW m}^{-1}$  are potentially available. As with electrical generation potential using ocean currents, the question becomes one of feasibility. Is there enough energy potentially available to justify the costs for extraction and can the technical challenges be met?

The commercial literature and commercial advocate group studies (e.g., McGowen et al., 2005) suggest that wave energy extraction is economically feasible for regions with energy flux per unit crest width greater than

$15 \text{ kW m}^{-1}$ . Two examples of devices under development are (1) a large snake-like set of linked cylinders that extract wave energy via undulations across a large linked cylinder length (e.g., 180 m for the 4-m diameter Pelamis WavePower device; <http://www.pelamiswave.com>) and (2) a 4-m diameter buoy that tracks the vertical motion associated with wave propagation past a fixed point (e.g., Ocean Power Technologies, Inc., <http://www.oceanpowertechnologies.com>). The first of these uses the length of the device to extract a major portion of the wave energy flux past the 4-m diameter cross section; the second of these is more limited in the percentage of the flux that can be extracted. Without questioning any of the details (see the industry brochures), it is clear that for either of these devices the total flux that may potentially be tapped is whatever passes the 4-m device width. So in either case, the question becomes: can some fraction of  $15 \text{ kW m}^{-1}$  times 4 m provide an economically feasible source of power (assuming that  $15 \text{ kW m}^{-1}$ , as promoted, is a viable level)? At best, assuming complete extraction with no losses (itself impossible),

devices such as these can garner at most  $60 \text{ kW}$ .

## Solar The Observations

Two of the COMPS buoys carried downward short-wave radiation sensors. Here we will use the most complete of these from mooring C10, located approximately 25 nm offshore from Sarasota, FL, where an Eppley PSP sensor was mounted as part of the IMET/ASIMET suite of air-sea interaction sensors. The veracity of these measurements for our purposes here follows from previous studies that utilized these data to diagnose the net surface heat flux and the associated variations on water column temperature (e.g., Virmani & Weisberg, 2003, 2005). Figure 10 provides these hourly sampled, solar insolation data that were collected approximately 2.5 m above the sea surface for the 8-year interval, from 1999 to 2007. On an hourly basis, we see that the daily maximum insolation varies from as high as  $1,000 \text{ W m}^{-2}$  in spring and summer to as low as  $500 \text{ W m}^{-2}$  in fall and winter. Averaging diurnally to account for the fact that there is no incoming short-wave radiation at night, we find highest daily mean values ranging from about  $300 \text{ W m}^{-2}$  in summer to  $150 \text{ W m}^{-2}$  in winter.

## Equivalent Energy Generation Potential Using Solar Panels

As with our analysis of wind energy generation, which recognized the maturity of the industry and hence allowed for us to choose a vendor with established product specifications, we do the same here for solar power. The example used is a Siemens SP75 solar panel. The method employed to determine the output of such a solar

**FIGURE 9**

Global wave energy flux per unit crest width (after McGowen et al., 2005).

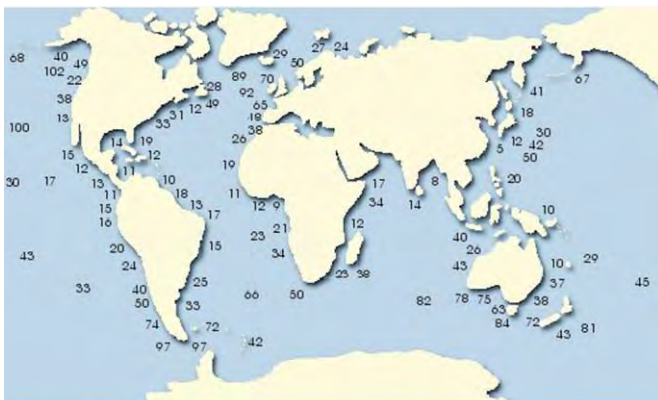
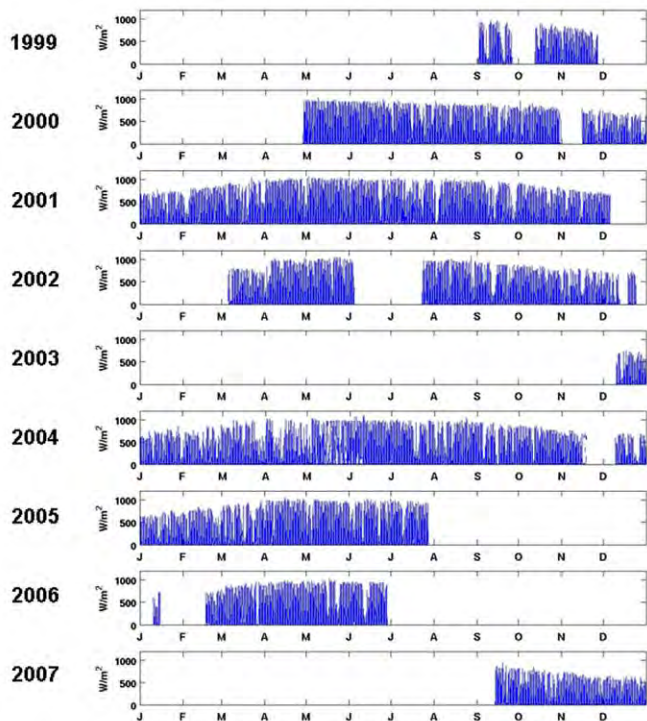


## FIGURE 10

Hourly sampled time series of incoming short-wave radiation measured 2.5 m above mean sea level at mooring C10 located approximately 25 nm offshore from Sarasota, FL. Shown are 8 years of observations spanning 1999 (top) through 2007 (bottom).



per unit area under WFS daily averaged insolation for this particular solar panel.

This technique (just demonstrated for an annually averaged diurnal cycle) was applied on a daily basis to convert observed incoming short-wave radiation to solar panel output normalized to a square meter. The results were then averaged diurnally to provide daily averaged power generation time series for the entire 8 years of record. Figure 12 shows the daily results, along with a climatological monthly mean time series (the bottom panel) obtained by averaging all of the Januarys, all of the Februarys, etc.

The daily averages range from essentially zero on strongly overcast days to  $40 \text{ W m}^{-2}$  on clear summer days. When averaged over the month we see a minimum in winter of about  $20 \text{ W m}^{-2}$  and a maximum in spring of about  $38 \text{ W m}^{-2}$ . The

panel is to calculate the equivalent number of hours for which such panel would capture insolation at a  $1,000 \text{ W m}^{-2}$  level. Thus, we computed an annual mean, hourly insolation curve for 2001 (the year for which our data are most complete) and integrated the area under that curve to arrive at an equivalent area (insolation  $\times$  time) at an insolation level of  $1,000 \text{ W m}^{-2}$  (Figure 11). Given that the Siemens SP75 solar panel is rated to output  $75 \text{ W}$  at an insolation of  $1,000 \text{ W m}^{-2}$ , we then determined the daily mean output for the device to be  $404 \text{ W h}$  (based on the equivalent solar production day of  $5.39 \text{ h}$ ). Dividing by  $24 \text{ h}$  gives  $16.8 \text{ W}$  as the average output for this annually averaged day, and dividing by the area of the solar panel ( $0.63 \text{ m}^2$ ) gives  $26.7 \text{ W m}^{-2}$  as the daily averaged power output

## FIGURE 11

The 2001 annually averaged daily insolation curve observed at C10 (blue) with equivalent number of hours at  $1,000 \text{ W m}^{-2}$  (black), where the areas under either of these distributions (blue or black) are the same.

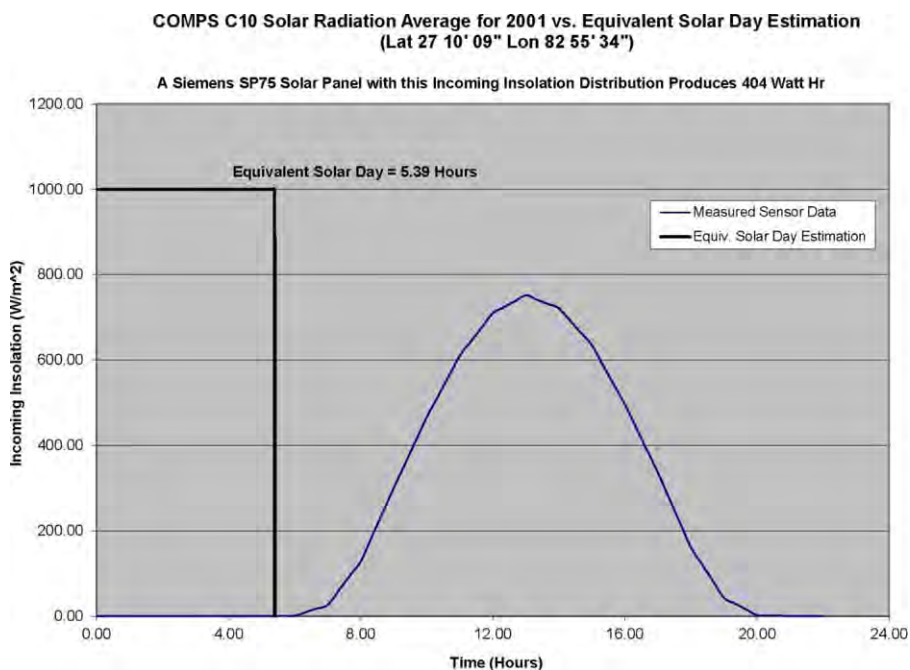
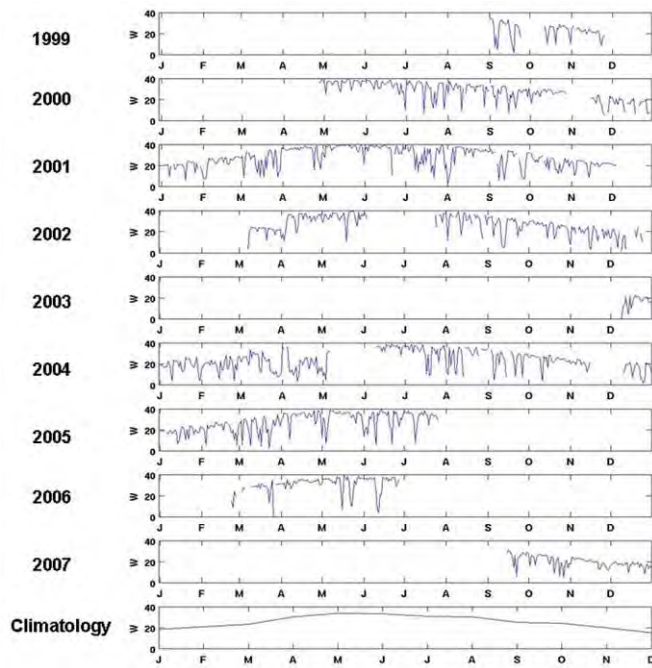




## FIGURE 12

1999 through 2007 time series of daily average solar panel output based on observed insolation from C10 and climatology.



average across the entire year is about  $25 \text{ W m}^{-2}$ .

## Discussion

Electrical power generation by windmills, solar panels, watermills (ocean current turbines), and wave devices have been topics of discussion for several decades. Wind and solar applications are mature, and commercial devices may be purchased and operated. Currents and waves applications have not reached a similar level of maturity. Devices exist and some have undergone field tests, but none are commercially viable yet. That in itself speaks to the relative utility of these concepts. The application of over a decade of coastal ocean observations from the WFS (augmented by model simulations) supports this viewpoint that alternative power generation from wind and solar sources appears to be more

promising than that from ocean currents and waves.

Further appreciation of this finding follows from a few simple economics considerations. We begin with the known cost for powering a modest home. As an example, consider a 2,000  $\text{feet}^2$  Florida apartment that consumes about 1.7 kW of electrical power on annual average at a cost of about \$140 per month or \$1,680 per year. If we were to transition from conventional fuels to wind power by deploying a machine equivalent to a GE 3.6 MW turbine, we would average 1 MW of production, sufficient (on annual average) to power 588 such homes. The present cost for powering these homes based on conventional fuels and rounded is \$1,000,000. A cost effectiveness transition to wind power would therefore require that the combined amortization, maintenance, energy storage, transmission

and distribution, salaries, general and administrative costs, plus shareholder profits be about \$1,000,000 per year for such a windmill. Whereas the specific costs for turbine purchase and installation are not readily available, anecdotal, nonrefereed literature suggests that these range between \$1.2 and \$2.6 million per MW of nameplate capacity. Thus, depending on the amortization of these capital costs, wind power may be approaching cost effectiveness. Support for this comes from an Associated Press article suggesting that the electrical delivery cost for a wind farm proposed offshore of Cape Cod, MA, will be roughly twice that by conventional fuels. So while the costs for electrical power generation by wind is higher than by conventional fuels, wind power generation may be economically feasible in the future, consistent with the fact that the wind power industry is indeed a mature one.

As with wind, it is difficult to find straightforward information on solar panel costs. Systems installation costs are estimated at about  $\$1,000 \text{ m}^{-2}$ , and with an annually averaged solar panel power production of  $26.7 \text{ W m}^{-2}$  by observed Florida insolation, the cost per watt would be about \$38. Thus, the solar panel cost for a modest 1.7 kW house would be about \$64,000, some 38 times the present annual cost of electricity by conventional fuels. This of course does not include any considerations of metering or storage strategies or properly sizing a system to actually meet user needs. While the above estimate may not be out of the realm of what may be reasonable based on amortization costs, any individual home owner would be hard pressed to justify such investment without a major subsidy.

The economics take a rapid turn for the worse when considering either



ocean currents or waves. Ocean currents, as discussed in Ocean Currents, require similar sized machines (watermills) as for wind, and the energy extraction potential is much more limited than for wind, even when considering a massive current like the Gulf Stream. Moreover, it would be impractical to deploy watermills of the same size as windmills; hence many more, much smaller watermills would be necessary than for windmills, greatly compounding the costs for an equivalent amount of energy. This is even before any consideration is given to the technical challenges of deploying and maintaining a large number of mechanical devices in a swift ocean current. From these arguments, we must conclude that alternative electrical power generation by ocean currents for any regional utility application would be both prohibitively costly and impractical. It is therefore not surprising that this industry remains in a developmental versus a mature stage.

Waves, in our opinion, are even more impractical than currents for utility scale power generation. Consider, for instance, either the approximate 4-m buoy or 180-m-long cylinder discussed in Ocean Waves. Even for seas with energy flux per unit crest width of  $15 \text{ kW m}^{-1}$ , these machines would have the potential to generate no more than 60 kW per machine, much less when necessary losses are considered. Using present electric costs as documented for a 1.7 kW house, 60 kW is worth about \$59,000 per year. Considering the need to swap out machines for servicing perhaps twice yearly, if not more frequently, it might cost more just for the ship time necessary to deploy and recover these machines than the value of the electricity that they could potentially generate and that does not

include any of the costs for purchasing the machines and establishing the infrastructure for their use.

In summary, the economics for alternative power generation by wind and solar means may result in cost-effective strategies in the future, whereas those for ocean currents and offshore waves will not, at least for projects in which large quantities of power are required, such as powering a major urban area. Other inhibiting considerations also come into play. Although our cost estimates are based on annually averaged quantities, it must be recognized that it is not uncommon for winds to be low enough to fail completely as an energy source (about 20% of the time on the WFS) and similar can be said of solar insolation. Thus, neither of these two potential alternative power-generation sources can fully replace power generation by conventional fuels; they can only supplement the use of conventional fuels.

Windmills of the type required to supplement large power needs are also massive in size. To provide a sense of spatial scale, a professional football stadium stood up on end provides an analogy to the equivalent cross sectional area that would be occupied by a large windmill. Accommodating such structures along highly populated coastlines would be difficult. Florida, with its highly developed, tourist-oriented, coastline would likely not be amenable to situating offshore utility-scale wind farms in sight of land. The use of solar panels in an array large enough to supplant a conventional facility also suffers from such matters of spatial scale. For instance, based on Florida insolation, replacing a 1.8-GW power plant, such as the Tampa Electric Company Big Bend facility (located on the east shore of Tampa Bay) would require  $90 \text{ km}^2$  of solar

panels, plus other storage devices required to accommodate evening hour or extended days of low insolation. Lacking installations of such massive scale, it remains unknown whether or not their maintenance would even be feasible.

## Conclusions

Based on analyses using coastal ocean observing system data for winds, incoming short-wave radiation and ocean currents, supplemented, as needed, by numerical model simulations, the following conclusions may be drawn. First, there are good reasons why industries pertaining to electrical power generation by the alternative means of wind and solar are much more mature than those pertaining to ocean currents and waves. Wind and solar sources of energy do provide promise for alternative power generation on a utility scale, whereas for many physical and practical reasons, ocean currents and waves do not. Second, even if wind and solar power in Florida are eventually produced in an economically competitive way (which requires a much more detailed economics analysis), these power sources may only be able to supplement power generation by conventional fuels or other means. They cannot replace presently required base load power-generation capacity.

## Acknowledgments

Sustained observations made this work possible. Initiated in 1998 with USF support from the Florida Legislature, COMPS has operated ever since by marshaling support from a variety of sources, including the U.S. Geological Survey, Minerals Management Service, Office of Naval Research,

National Oceanic and Atmospheric Administration, the Florida Department of Community Affairs and the Florida Wildlife Commission, recent support (in addition to USF) being through the Office of Naval Research grants N00014-05-1-0483 and N00014-10-1-0785, NOAA ECOHAB grant NA06NOS4780246, NOAA IOOS grant NA07NOS4730409, and NSF grant OCE-0741705. Specific to this application is also a grant from the Florida Energy Systems Consortium (FESC). Data collection success is owed to COMPS staff, with seagoing operations by J. Law and (formerly) R. Cole, data analysis, management and quality assurance by J. Donovan, D. Mayer and P. Smith, and engineering assistance through the CMS Center for Ocean Technology, in particular R. Russell. Prof. S. Shin assisted with the NAM boundary layer winds.

## Corresponding Author:

Robert H. Weisberg  
College of Marine Science,  
University of South Florida  
140 7th Ave. S., St. Petersburg,  
FL 33701  
Email: [weisberg@usf.edu](mailto:weisberg@usf.edu)

## References

- Betz**, A. 1920. Das Maximum der theoretisch möglichen Ausnutzung des Windes durch Windmotoren, Zeitschrift für das gesamte Turbinenwesen. 20. September 1920.
- Chassignet**, E.P., Hurlburt, H.E., Smedstad, O.M., Halliwell, G.R., Hogan, P.J., Wallcraft, A.J., ... Bleck, R. 2007. The HYCOM (HYbrid Coordinate Ocean Model) data assimilative system. *J Marine Syst.* 65:60-83. <http://dx.doi.org/10.1016/j.jmarsys.2005.09.016>.
- Chassignet**, E.P., Hurlburt, H.E., Metzger, E.J., Smedstad, O.M., Cummings, J., Halliwell, G.R., ... Wilkin, J. 2009. U.S. GODAE: Global ocean prediction with the HYbrid Coordinate Ocean Model (HYCOM). *Oceanography*. 22:48-59. <http://dx.doi.org/10.5670/oceanog.2009.39>.
- Large**, W.G., & Pond, S. 1981. Open ocean momentum flux measurements in moderate to strong winds. *J Phys Oceanogr.* 11:324-36. [http://dx.doi.org/10.1175/1520-0485\(1981\)011<0324:OOMFMI>2.0.CO;2](http://dx.doi.org/10.1175/1520-0485(1981)011<0324:OOMFMI>2.0.CO;2).
- Leaman**, K.D., Molinari, R., & Vertes, P. 1987. Structure and variability of the Florida vurrent at 27N: April 1982–July 1984. *J Phys Oceanogr.* 17:565-83. [http://dx.doi.org/10.1175/1520-0485\(1987\)017<0565:SAVOTF>2.0.CO;2](http://dx.doi.org/10.1175/1520-0485(1987)017<0565:SAVOTF>2.0.CO;2).
- Liu**, Y., & Weisberg, R.H. 2005. Patterns of ocean current variability on the West Florida Shelf using the self-organizing map. *J Geophys Res.* 110:C06003. <http://dx.doi.org/10.1029/2004JC002786>.
- Liu**, Y., Weisberg, R.H., Merz, C.R., Lichtenwalner, S., & Kirkpatrick, G.J. 2010. HF radar performance in a low energy environment: CODAR SeaSonde experience on the West Florida Shelf. *J Atmos Oceanic Technol.* 27(10):1689-710. <http://dx.doi.org/10.1175/2010JTECHO720.1>.
- McGowen**, C., Bedard, R., & Lenssen, N. 2005. Ocean tidal and wave energy, renewable energy technical assessment guide-TAG-RE, EPRI, Palo Alto, CA, 2005, 1010489.
- Niiler**, P.P., & Richardson, W.S. 1973. Seasonal variability of the Florida current. *J Mar Res.* 31:144-67.
- Stommel**, H.M. 1965. The Gulf Stream: a physical and dynamical description. Berkeley, CA: University of California Press. 248 pp.
- Tolman**, H.L. 1991. A third-generation model for wind waves on slowly varying, unsteady and inhomogeneous depths and currents. *J Phys Oceanogr.* 21:782-97.
- Tolman**, H.L. 1999. User manual and system documentation of WAVEWATCH-III version 1.18. NOAA / NWS / NCEP / OMB Technical Note 166. 110 pp. [http://dx.doi.org/10.1175/1520-0485\(1991\)021<0782:ATGMFW>2.0.CO;2](http://dx.doi.org/10.1175/1520-0485(1991)021<0782:ATGMFW>2.0.CO;2).
- Tolman**, H.L. 2010. WAVEWATCH III (R) development best practices Ver. 0.1. NOAA / NWS / NCEP / MMAB Technical Note 286, 19 pp.
- Virmani**, J.I., & Weisberg, R.H. 2003. Features of the observed annual ocean-atmosphere flux variability on the West Florida Shelf. *J Climate.* 16:734-45. [http://dx.doi.org/10.1175/1520-0442\(2003\)016<0734:FOTOAO>2.0.CO;2](http://dx.doi.org/10.1175/1520-0442(2003)016<0734:FOTOAO>2.0.CO;2).
- Virmani**, J.I., & Weisberg, R.H. 2005. Relative humidity over the West Florida Continental Shelf. *Mon Weather Rev.* 133:1671-86. <http://dx.doi.org/10.1175/MWR2944.1>.
- Weisberg**, R.H., He, R., Liu, Y., & Virmani, J.I. 2005. West Florida shelf circulation on synoptic, seasonal, and inter-annual time scales. In *Circulation in the Gulf of Mexico*, W. Sturges and A. Lugo-Fernandez, eds., AGU monograph series. Geophysical Monograph. 161:325-47.
- Weisberg**, R.H., Barth, A., Alvera-Azcárate, A., & Zheng, L. 2009. A coordinated coastal ocean observing and modeling system for the West Florida Shelf. *Harmful Algae.* 8:585-98. <http://dx.doi.org/10.1016/j.hal.2008.11.003>.